Energy Assessment of a Parabolic Trough Collector in North Cyprus

Olopade Olusegun Solomon

Submitted to the
Institute of Graduate Studies and Research
in partial fulfillment of the requirements for the Degree of

Master of Science
in
Mechanical Engineering

Eastern Mediterranean University
November 2011
Gazimağusa, North Cyprus

Approval of the Institute of Graduate Studies and Research

Prof. Dr. Elvan Yılmaz
Director

I certify that this thesis satisfies the requirements as a thesis for the degree of Master of Science in Mechanical Engineering.

Assoc. Prof. Dr. Uğur Atikol
Chair, Department of Mechanical Engineering

We certify that we have read this thesis and that in our opinion it is fully adequate in scope and quality as a thesis for the degree of Master of Science in Mechanical Engineering.

Assoc. Prof. Dr. Uğur Atikol
Supervisor

Examining Committee

1. Prof. Dr. Hikmet Aybar _____

2. Assoc. Prof. Dr. Fuat Egelioğlu _____

3 Assoc. Prof. Dr. Uğur Atikol _____

ABSTRACT

The present work is concerned with the investigation of the performance of a parabolic trough collector in North Cyprus. The Feasibility of using this collector for the purpose of supplying hot steam in a solar thermal power plant has been the interest of energy policy makers recently. In order to optimize the performance of trough, a mathematical simulation was carried out displaying the temperature of the out flowing working fluid. The simulation results show that the temperature of the working fluid exiting a trough ranges from 80 ^{0}C to 115 ^{0}C during the summer months and is less than 80 ^{0}C during winter. This shows that using parabolic trough mirror for setting up a concentrating solar plant in North Cyprus is technically feasible.

Keywords: Concentrating Solar Power, Parabolic Trough, System Simulation, Collector size.

ÖZ

Bu akademik çalışma Kuzey Kıbrıs'ta parabolik güneş kollektörlerinin performansını araştırmakla ilgilidir. Son zamanlarda güneş enerjisi kollektörlerinin kullanılarak güneş termik santrallerinde sıcak buhar temin etmesinin ulaşılabilirliği konusu , enerji politikası ile ilgilenenlerin ilgi odağı olmuştur. Güneş kollektörlerinin performansını optimize etmek için, dışarı akan akışkanın sıcaklığını ölçmeye yarayan matematiksel simulasyon oluşturuldu. Bu simulasyonun sonuçlarına göre, dışarı çıkan akışkanın sıcaklığı yaz aylarında 80-115 derece, kış aylarında ise 80 derece nin altındadır. Bu değerler bize gösterdi ki, Kuzey Kıbrıs'ta parabolik güneş panelleri kurmak teknik olarak uygundur. Ancak, bu sistemin kurulum maliyeti oldukça yüksek ve bu panellerin ömürleriyle ilgili,

Anahtlar kelemiler: Güneşsel konsantre olan güç, parabolic yemliği, Sistem takliti, Koleksiyoncu oylumu.

I dedicated this thesis to Almighty God, who gave me the grace to be able to complete it.

ACKNOWLEDGMENTS

Above all, I would like to thank God for giving me the opportunity of being here, at this precise time and moment.

I want to sincerely thank Assoc. Prof.Dr.Ugur Atikol for giving me the opportunity of working under his guidance and for his contribution towards the success of my thesis. This work is today a reality, thanks to his unconditional help and guidance. I will be forever grateful. It has been my dream, for several years, to be able to contribute in the renewable energy field. I also want to express my gratitude to Mr. Agboola Philips (PhD in view) and my simulation Programmer Orxan Shibliyev for sharing their vast knowledge with me.

And last, but certainly not least, I want to thank my Family and the church of God CPEM Bethesda for their support in prayers and kindness.

TABLE OF CONTENTS

LIST OF TABLES

LIST OF FIGURES

NOMENCLATURE

ABBREVIATIONS

BBER	Bureau of Business and Economic Research
CSP	Concentrating Solar Power
CO_2	Carbon dioxide
DLR	Deutsches Zentrum Fur Luft und Raumforte
DNI	Direct Normal Radiation
HTF	Heat Transfer Fluid
SEGS	Solar Electric Generation System

Symbols

a	Width of the aperture.
a_0	Gap width (m).
A_a	Area of aperture (m^2).
A_r	Area of receiver (m^2).
C	Concentration ratio
$C_{1,}$ C2, C3	Constant.
C_p	Specific heat,(kJ/kg-K).
D	Dispersion angle (Degree).
D_i	Receiver inner diameter (m)
D_0	Receiver outer diameter (m)
F	Friction factor
F’	Collector efficiency factor

F_R Collector heat –removal factor.

h Heat transfer coefficient (W/m^2-K).

$h_{r,r-c}$ Natural convective heat transfer coefficient.

$h_{r,c-a}$ Radiation coefficient between the cover and the ambient air equation.

h_w Wind heat transfer coefficient, (W/m^2-K).

I_b Beam radiation on a horizontal surface (W/m^2).

I_{bn} Beam radiation on a surface normal to the direction of the rays, (W/m^2).

I_d Diffuse radiation on a horizontal surface (W/m^2).

I_T Flux incident on top cover of collector on aperture plane (W/m^2).

k thermal conductivity, (W/m-K).

K Extinction coefficient, (m^{-1}).

L Space between absorber plate and cover (m)

m mass flow rate, (kg/s).

n Day of the year.

N Number of modules

N_u Nusselt number

Pr Prandtl number

R_b Tilt factor for beam radiation.

R_d Tilt factor for diffuse radiation.

R_r Tilt factor for reflected radiation.

S Incident solar flux absorbed in the absorbed plate or tube, (W/m^2)

t Time (s)

T Temperature, (^{0}C)

T_a ambient Temperature, (^{0}C)

T_{fi} Temperature of fluid at inlet, (^{0}C)

T_{fo} Temperature of fluid at outlet, (^{0}C)

T_{fm} Mean absorber surface temperature, (^{0}C)

U_L Velocity, (m/s)

Greek Symbols

α Absorptivity of absorber surface for solar radiation (m^2/s)

α_n Absorber normal radiation

β Slope or Tilt

γ Surface azimuth angle, intercept factor.

δ Declination

ε_c Cover emissivity

ε_r Receiver emissivity

η Efficiency

θ, θ_1 Angle of incidence

θ_2 Angle of refraction

θz Zenith angle

μ Viscosity, (N-s/m^2)

υ Kinematic viscosity, (m^2/s)

ρ Reflectivity, Density, (kg/m^3)

σ Stefan-Boltzmann constant, (W/m^2-K^4)

τ Transmissivity of cover or covers,

τ_a Transmissivity based on absorption

τ_r Transmissivity based on reflection and refraction

ϕ Latitude

ϕ_r Rim angle

ω Hour angle

Chapter 1

INTRODUCTION

Each year over 1 billion terawatt hours of solar energy reaches the earth surface [1]. This corresponds to about 60,000 more than the world's current electricity demand, thus solar power has the biggest potential of all renewable energies. This ample sufficiency of solar energy makes solar power plants an alternative to traditional power plants which burn polluting fossil fuels such as oil number six. Solar power plants incorporate concentrating mirrors for collecting as much solar energy as possible, and are known as concentrating solar power (CSP) plants. These concentrated solar power systems provide favorable environmental benefits since they produce virtually no emissions and consume no fuel except for sunlight. The CSP impact on environment is on land use [2]. The amount of land occupied by the CSP plants is considerably more than that of fossils fuel plant. The use of solar plant is not recent, however In 1907 Germany was granted the first patent of solar collector [3].

North Cyprus is an island with a population over 260,000, located at 35^0 N of the equator and 33^0 E of Greenwich. Its land area is about 3354km^2. The island is a typical Mediterranean area characterized by hot and dry summers and mild winters. The average temperature during summer and winter seasons are 28^oC and 11^oC respectively [4]. Energy production, transmission and distribution in north side of the island are under responsibility of Cyprus Turkish Electricity Authority (KIB-TEK). Total generation

capacity of KIB-TEK is 346.3MW as at 2011, and it is entirely dependent on oil and petroleum products [5, 6]. The use of fossil fuel driven electricity plants causes effects on environment and can be a burden on the economy of the country. Although one cannot deny that the exploitation of fossil fuels had advanced civilization and industrialization, the recent concern on the degradation of the environment and climate changes sets limitation in the future welfare for mankind. Therefore, new resources must be introduced to strike a balance. North Cyprus has no oil resources, but has alternative energy resources such as solar energy which can help in diversifying the energy options of the country besides oil and natural gas. For this reason, the use of concentrating solar collectors can be used as part of the renewable energy alternatives for the production of electricity.

The present work will focus on the optical and thermal analysis of a parabolic trough collector under the climatic conditions of North Cyprus. This can be done by modeling the trough theoretically to derive the temperature outputs of the working fluid for different months.

The objectives of this present work are.

1) To analyze the viability of the parabolic trough collector through a simulation model, taking solar transient conditions into account.
2) To examine the theoretical approach of parabolic trough model, taking into consideration the optics and heat transfer fluid. This analysis was conducted in Microsoft Excel to provide the opportunity of altering or changing system components.
3) To determine the temperature outputs of the working fluid from a parabolic trough collector under the climatic conditions of North Cyprus.

4) To determine hourly performance of the parabolic trough system under the solar transient of North Cyprus.

Chapter 2 discusses the description of technologies and the use of CSP around the world.

Chapter 3 describes the parabolic trough collector model, its geometry and it explains the optical analysis associated with it.

Chapter 4 presents the solar radiation, performance parameters, the simulation results obtained during the solar transient analysis.

Chapter 5 states the conclusion and proposed recommendations.

Chapter 2

A REVIEW OF THE CSP TECHNOLOGIES

2.1 Description of CSP Technology

2.1.1 Introduction

Concentration of solar radiation is achieved by using a reflecting arrangement of mirrors or a refracting arrangement of lenses. The optical system directs the solar radiation on to an absorber of smaller area which is usually surrounded by a transparent cover. Because of the optical system, certain losses (in addition to those which occur while the radiation is transmitted through the cover) are introduced. These include the reflection or absorption losses in the mirrors or lenses and losses due to the geometrical imperfections in the optical system. The combine effect of all such losses is indicated through the introduction of a term called the *optical efficiency* [7]. The introduction of more optical losses is compensated for by the fact that the flux incident on the absorber surface is concentrated on a smaller area. As a result, the thermal loss terms do not dominate to the same extent as in a flat plate collector and the collection efficiency is usually higher.

It has been noted earlier that some of the attractive features of a flat plate collector are simplicity of design and ease of maintenance. The same cannot be said of concentrating collector usually has to follow or track the sun so that the beam radiation is directed onto the absorber surface. The method of tracking adopted and precision with which it has to

be done varies considerably. In collectors giving a low degree of concentration, it is often adequate to make one or two adjustment of the collector orientation every day and it can also be done manually. On the other hand, with collectors giving a high degree of concentration, it is necessary to make continuous adjustments of the collector orientation. The need for some form of tracking introduces a certain amount of complexity in the design. Maintenance requirements are also increased. These entire factors add to the cost. An added disadvantage is the fact that much of the diffuse radiation is lost because it does not get focused [8].

In the last few years, significant advances have been made in the development of concentrating collectors and a number of types have been commercialized abroad. Almost all of them are the line focusing type like parabolic trough collectors, and yield intermediate temperatures. Typical efficiencies obtained with such collectors range between 40 and 60 per cent at delivery temperature of 150^{o}C to 200^{o}C. These values are generally higher than those obtained with conventional flat plate collectors at lower delivery temperatures [8].

2.1.2 Concentrating Solar Collectors

Concentrating solar collectors are required when higher temperatures are needed. By decreasing the area from which heat losses take place energy delivery temperature can be increased. The energy absorbing surface and an optical device between the sources of radiation can be done by interposing [9]. Solar collector array can be classified as, concentrating or non-concentrating, reflecting or refracting, imaging or non-imaging, linear, focal or central, tracking or fixed etc. Collectors can be further described in terms

of: their concentration ratio, thermal and optical performance, heat transfer capability, and overall efficiency [10, 11, 12].

Concentrating Solar collectors are heat exchangers that use solar radiation to heat a working fluid, usually a liquid or air. They are classified as focusing collectors, which must ‘track’’ the sun and can generally utilize only the direct radiation. They are capable of producing high temperature [13].Different applications are dependent on (space heating or water, steam production or electricity generation), there are different requirements as to the temperature the collector system can achieve [10]. This fact regularly decide if the collector need be concentrating for attaining higher temperatures or non-concentrating, for lower temperature applications. The major important classification about feasibilities lies on the collector. Concentrating solar collectors for electricity production valid today are of the imaging type. NREL recently guided a study concerning different collector materials [14]. The significant of science for non-imaging optics is based with the optimal transfer of light radiation in the middle of a source and a target, not in forming an image of the source, but like imaging optics. A non-imaging optic system particularly improves at concentrating and illuminating than their imaging counterparts [10]. The flux at the surface of the Sun is approximately 63,000 kW/m2 [11].It decays with the square of the distance from the Sun to the Earth to a value of 1.370 kW/m2 just above the Earth’s atmosphere, and typically to 0.8 - 1 kW/m2 at the ground. An optical device to concentrate the solar flux to obtain temperatures at the earth's surface not transcending the sun's surface temperature permitted by second law of thermodynamics . In practice, flux concentration fall short because imaging optical contrives are inefficient at delivering maximum conventional means [15]. Non-imaging light-gathering devices can increase in quality on focusing designs by a factor of four or

more, and access the thermodynamic limit. The non-imaging design is capable to concentrate terrestrial sunlight by a factor of 56,000 to manufacture an irradiance that could exceed that of the solar surface [11].

There are four typical types of concentrating solar power systems: parabolic troughs, central receiver systems, dish/engine systems and Fresnel reflector systems. These technologies can be utilized to generate electricity for a diversity of applications ranging from remote power systems as small as a few kilowatts up to grid-connected applications of 200-350 megawatts or more.

2.1.2.1 Parabolic Trough System

Parabolic trough systems consist of parallel row of large reflective parabolic troughs that focus solar energy onto a central receiver piper (also called ‘absorber pipe’’ or heat collector element) placed at the focal line of the parabolic surface. The receiver is designed to be capable of absorbing the energy concentrated on it and it should be capable to restrain the outcome of high temperature. Purposely the receiver are made of steel tubing with a black coating surrounded with a protective glass cover, in between is the space of two evacuated to reduce heat loss [16]. The outer glass surface maybe supplemented with anti-reflective coating to intensify efficiency more. The heat collected from the parabolic troughs are run through the pipes in the direction of the length of each solar trough is synthetic oil, alike to engine oil, and is able to operate at high temperature. While the operation it is likely to reach between 300 ^{o}C and 400 ^{o}C and run through the heat exchanger where the steam is extracted from heat and is used to drive a steam turbine generator to supply electricity. The heat transfer fluid recycled over and over through the solar collector field to gain more heat as shown in the Fig 2.1.

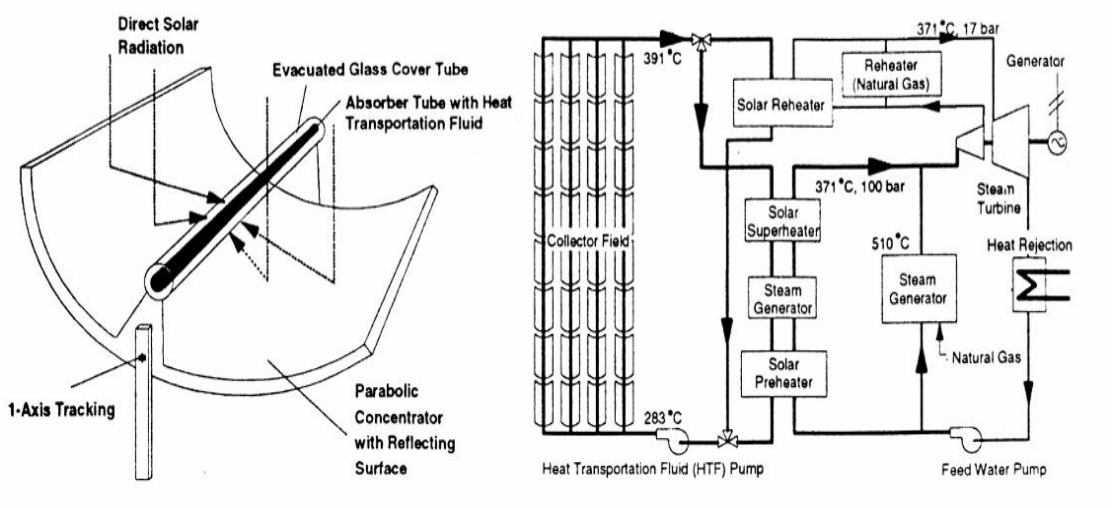

Fig 2.1: Schematic of Parabolic Trough and Power Plant of SEGS Type [17]

The parabolic troughs are in different sizes, the receiver run maybe 5-6m wide, 150m in length and up to 1 or 2 m deep. Large numbers of these are needed to collect enough heat to supply for a single power plant.

Parabolic are mostly used to generate steam for a Rankine cycle. They are currently the most proven electricity generating technology by solar means. There are nine large commercial-scale solar power plants that have been operating in the Californian Mojave Desert Since 1984. These nine solar energy generating systems (SEGS) are the largest solar energy generating facility in the world and range in power outputs from 14 to 80MW, in total 354MW of installed capacity. They are located in Californians' Mojave Desert, where insolation is among the best in the United State (U.S). The facilities have a total plant displace 3800 tonnes of pollution per year, power 232500 homes and displace 815,000 barrels of oil annually. The plants use parabolic trough technology along with the natural gas to generate electricity. 90% of the electricity is produce by sunlight and 10% is produced by natural gas [14, 15].

2.1.2.2 Parabolic Tower System

The solar tower system are usually called solar central receive power plants is another option to take advantage of energy from the sun. Heliostat is a device in power a tower system, which tracks the position of the sun that is used to direct a mirror of field of mirrors, during the day, to reflect sunlight onto a target-receiver to collect energy from the sun. The receiver formed to take in energy from the sunlight incident on it and transfer it through the heat transfer fluid. The heat transfer may be molten Salt, water or air. This energy is then passed either to the storage or to power-conversion systems, which convert the thermal energy into electricity. Heliostat field, the heliostat controls, the receiver, the storage system, and the heat engine, are the major components of the system which drives the generator. Solar tower energy storage is designed to operate for 24hours a day [18].

Parabolic tower technology cost is expensive but it has higher temperature to produce higher efficiency generation. In 2003, [19] suggested that in the medium to long term this might become the lowest cost form of solar power such system is shown in Fig.2.2.

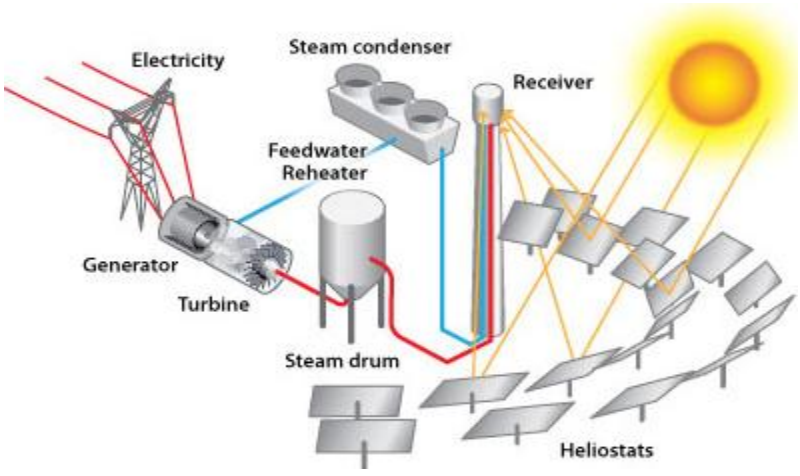

Fig 2.2: Schematic drawing of solar tower [20]

2.1.2.3 Parabolic Dish System

The parabolic dish system utilize a parabolic dish shaped mirror or a modular mirror system that approximates a parabola and combine two-axis tracking to focus the sunlight onto receivers situated at the focal point of the dish which absorbs the energy and converts it into thermal energy [21] as it take focus show in Fig 2.3. The system collects the solar energy radiating directly from the sun into a receiver to heat a fluid or gas (air) to approximately 750^{o}C. Heat engine located at the focus is used to generate heat from concentration to supply mechanical motion that propelled the generator. A parabolic solar dish engine is called stirling engine with very high efficiency. A small gas turbine based on brayton cycle were attempted to be use [22]. Parabolic solar dishes has standard of 5m and 10m in diameter and a reflective areas 40-120m^2 which has been built as large as 400m^2. About 50kW power size range could be provided by dishes. But, stirling engines power are narrow to 25kW. Gas turbine heat engine with micro-turbines supply higher output but they are importantly less efficient than stirling engines. Stirling engine and micro-gas turbine systems can be design for hybrid operation using combustion of solar heat and the heat from combustion of natural gas [23]. In line with both parabolic troughs, solar dishes collectors and heliostats should be able to track the sun for maximum efficiency.

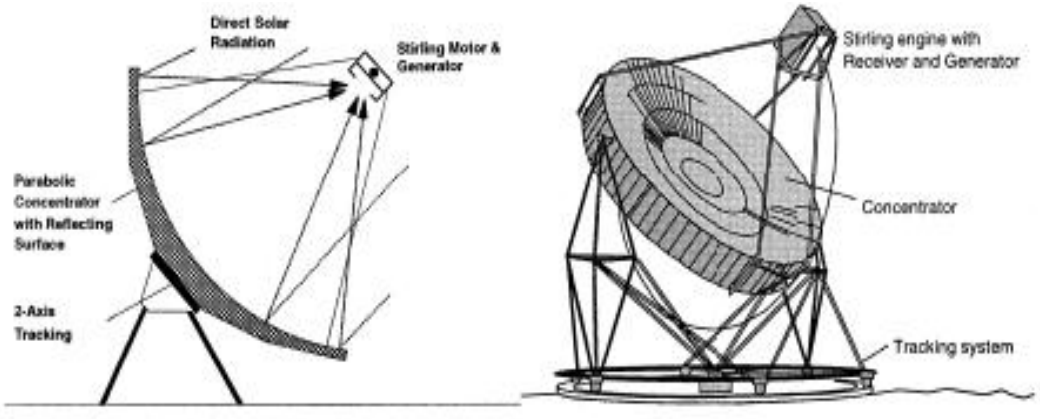

Fig 2.3: Schematic of parabolic Dish [16]

2.1.2.4 Fresnel Reflector

The Fresnel mirror type of CSP system is extensively alike to parabolic trough systems but as a replacement of using trough- shape mirrors that track the sun. It uses long flat mirror at various angles that have the effect of focusing sunlight on one or more pipes include heat collecting fluid which are mounted above the mirrors. The comparative plainness of this type of system means that it is likely to be relatively cheap to manufacture and lighter optical systems, while this will probably have lower energy conversion efficiency and may not have the high optical accuracy of dish and trough systems.

Fresnel solar collector is based on a development of this concept where a number of discrete mirrors approximate a large parabolic trough collector are used on solar troughs and dishes and does not require flexible connection between the receiver and the piping systems that carry heated fluid or steam to the centralized boiler or engine. This is shown in Fig 2.4.

Fig 2.4: A picture diagram of a Fresnel reflector [16].

Table 1: Comparison of CSP Technologies [21]

TABLE-I : COMPARISON OF CSP TECHNPLOGIES [21]

Parameter	Solar Thermal (CSP) Technologies			
	Parabolic Trough	Solar Tower	Fresnel Reflector (CFLR)	Solar Dish
Site Solar Characteristics/ Solar radiation required	Generally sites with annual sum of DNI larger than 1800 kWh/m²			
Land Requirement	Typically 5-7 acres/MW			
Typical shape of solar plant	Rectangle	Sector of a circle/ Rectangle	Rectangle	Rectangle
Water Requirement	Typically $4m^3$/MWhr			No water requirement
Maximum Temperature	400 deg C	270 deg C Possible upto 560 deg C	400 deg C	800 deg C
Efficiency	~ 14%	~17% Possible upto 22%	-	~ 22-24%
Typical CUF	Typically 22-25%			
Plant cost		Lower than parabolic trough	Lower than parabolic trough	Very High
Largest plant size	80 MW	20 MW	5 MW	
Development Status	Most proven	Mature	Demonstration	Demonstration
Plants installed	-9 SEGS plants (14 MW to 80 MW) in California built from 1985 to 1991 – Total capacity : 354 MW - Nevada Solar One (64 MW) started in 2007	-Planta Solar 10 and Planta Solar 20 are in operation with capacities of 11 and 20 MW in Seille Spain -Sierra Sun Tower USA 5 MW - Solar Two plant (10 MWe) with molten salt storage-demo plant	- 9MWth used for FW heating in 2000 MW coal fired Liddell Power plant (Australia) - Two small capacity experimental plants in Spain in 2007 - 1.4 MWe at Murcia, Spain in 2009	Small operational plants with unit size of 10-25 kW
Technology Providers	Sener Solar Millenium Abengoa ACS-Cobra Acciona Solel	Abengoa eSolar Sener BrightSource Torresol Solarreserve	Austra MAN Ferrostaal	Stirling Energy Systems

2.2 CSP around the World

CSP technologies require more research to subdue non-technical and barriers. In two century ago the issue of climate change is not a concern. But in the early stage of industrial revolution the climate change has been a great worried. The ongoing depleting of fossil energy resources produced a solid momentum for market diffusion of renewable energy sources and their corresponding conversion technologies [18]. In a process to convert solar energy design utilizable for human obligation there are distinct pathways [18]. Usually, heat, electric energy, kinetic energy and chemical energy can be supplied by means of solar energy conversion. Concentrating solar power plant (CSP) plants convert direct solar irradiance into electricity [24]. Appropriate site for CSP plants are situated around the world. However, CSP is still a good position application for today's global substitute but installation of new CSP plant display high development rate [25]. Based on satellite data, potential CSP site are grouped and a worldwide distribution of high attribute potential CSP site is extracted. Also to CSP, new research shows that large scale photovoltaic (PV) power plant in Middle East and North Africa (MENA) region may lead to similar electric and economic attribute referring to conventional CSP plants [26]. This section will briefly describe the attainable solar thermal plant both in operation and under construction around the globe.

2.2.1 CSP Project in operation

2.2.1.1 Solar Electric Generation System (SEGS)

Solar Electric Generating System (SEGS) is a well known solar energy generation device in the globe. "It is made up of nine solar power plants, situated at Mohave Desert in Californian, USA with almost 2700 kWh/m^2 solar potential per annual". "The entire plant installed is 354 MW capacities with an average gross solar output for all nine

plants at SEGS is about 75 MW_e" .which amount it to be to the widest installation of solar plant of any class in the world. More so, at night the turbines can be used while burning the natural gas. The total solar field area of the parabolic reflecting mirror is more than 6,400,000m^2 arranged a rows, the parabolic mirror is enlarge more than 370km. The installation of SEGS utilizes parabolic trough together with natural gas to produce electricity. Almost 90% of the electricity is generated by the sunlight when the solar power is insufficient, natural gas is only used to gain the electricity required to southern Californian. "The installation of the working fluid (HTF) uses synthetic oil which heat to over 400 ^{0}C and drives the rankine cycle steam turbine by means of generating electricity" [27].

2.2.1.2 Andasol 1and 2

"This is the first solar thermal parabolic trough power plants to operate in Europe which is situated in Andalucía Spain" .These two solar thermal plants are exactly alike. "The Andasol 1 plant has three segments which are the solar field, the storage tanks and the power generation block". "Andasol plant uses solar field of about 642 parabolic mirrors ordered in 150loops with entire area of reflective is more than 510,000m^2 in a land area of 2,000,000m^2". "The annual electricity generation was estimated to provide 179 GWh with 2201 kWh/m^2 annual solar potential". "The annual average solar field efficiency estimated about 43%, while the steam efficiency is about 38.1% and 16% of overall plant efficiency" [28].

Andasol plant was the first to use two heat storage tank of molten salt for lower solar energy. The use of heat storage commences at the noon, when sun irradiation is high and it generates electricity at the same time charging the storage tank. The heat from the HTF (molten salt) charges the storage system and amasses till it is full. When heat is

released the molten salt cools down and transfer to the cold tank. The two-tank system exists for both the cold and the hot tanks. The storage tank diameter is 36m and 14m height of each and 7.5 hours storage capacity for 50 MW. The molten salt quantity employed estimated 28,500tonnes and a melting point of 223 ^{0}C. The permitted operational temperature is between 291 ^{0}C (cold tank) and 384 ^{0}C (hot tank) [28].

2.2.1.3 Nevada Solar One collectors

Parabolic trough technology is the only trough used at the Nevada solar one plant. The Valley of El Dorado is situated in Nevada, USA. It has 760 solar parabolic troughs with reflective surface each of 470m^2. To sum up, a total of 357,200m^2 of solar field reflective and about 160000m^{2}area of land are used. "The capacity of the steam turbine generate up to 64MW and annually the plant produces 130 GWh while additional gas heater is used for the back-up steam generation in case of inadequate of solar irradiation"[29]

2.2.1.4 PS10

PS10 solar thermal plant is an operational plant that used solar tower technology and it is situated at sanlucar de Mayor in Sevilla, Spain and started operation in 2007. PS10 is the first to use solar tower power plant to start commercial electricity generation operation in the world with 600000m^2 area of land. The solar tower is 100m high, and the tracking devices (Heliostat) that track the sun in two axes. The focal part (receiver) is connected at the sun's irradiation located on the tower with about 624 solar towers with surfaces area of 120m^2 each. Hence the total reflected surface area is 75000m^2. The solar radiation is directed towards the receiver with the use of solar tracking mechanism (Heliostat) [29].

The annual solar potential is about 2100kWh/m^2 and capacity of 11MW is installed, the plant is able to generate 24.3GWh of electricity annually. It stores 1h worth of steam for electricity generation by means of steam storage tanks. “The steam is stored at 50bar and 285 ^{0}C the sum of the plant efficient is nearly 17%”[29].

2.2.2 CSP thermal plant under construction

2.2.2.1 Solnova 1

This is a large concentrating solar thermal plant to be invent in the Sanlucar de Mayor situated in Sevilla, Spain. It utilizes parabolic trough technology. “The plant working fluid is the synthetic oil to produce high temperature steam and run a convectional steam cycle”. “The plant will include of 90rows of collectors directed north-south. Each row will have four trough modules (Hence a total of 360 modules) with 12.5m long and 5.75m wide while every module will rotate about it axis to track the sun” [30]. Adequate space will be left between the rows to lesson losses due to shading and enable for easy operation and maintenance. The surface total reflective will be calm approximately 260,000m^2 of mirrors. The whole area of the solnova 1 plant amounted to 1,200,000m^2. It installed about 50MW capacity to generate 114.6 GWh of clean electricity energy annually. The plant will be able to make up to 12-15% capacity by means natural gas combustion in case of low solar radiation conditions. “At peak point the plant will convert solar radiation to heat at 57% efficiency and join with the 34% efficiency of the steam cycle and the efficiency of the overall plant is estimated to be 19% approximately” [30].

2.2.2.2 PS20

“Is a solar thermal power plant still in the process of construction, it has technology pattern to PS10. It is constructed in line with the PS10 plant but with double capacity of

20MW. It will have about 1225 tracking sun heliostats each with a surface are of 120m and the solar tower has about 160m long. PS20 is expected to be capable to generate 48.6GWh per year, with entire land requirement of 900,000m^2."It will have the feasibility to burn natural gas to cover 12-15% capacity when there is low solar irradiation"[30].

2.2.2.3 Solar Tres

Construction of solar tres solar thermal plant in Andalucía Spain is still in progress. Solar tower was used for the thermal plant with a capacity of 19MW. "Solar Tres will use 2480 heliostats for the entire reflective surface area of approximately 300,000m^2 situated in a land of 1,420,000m^2 and the level of annual solar potential reaches 2060kWh/m^2"[44]. A rare display of solar Tre plant is the utilization of molten salt as a heat transfer medium in the interior of the receiver in place of the heat transfer fluid (synthetic oil) usually used in solar thermal power plants. Solar Tres plant will use enormous thermal storage system by using 6250tonne of salt with insulated storage tank heater immersion. The high capacity liquid nitrate salt storage system is at low-risk and efficient and is formulated for a high-temperature liquid salt at 565 ^{0}C and a cold temperature salt at 45 ^{0}C over its melting point (240 ^{0}C). "The design of the solar Tres will use 43MW steam generator system that will have a forced recirculation steam drum The storage system may supply back-up steam for up to extra 15h"[30].

2.3 Extensive Comparison

The prime attention for solar thermal plants is the quantity of land required, that is important. The land area needed depends on the solar potential availability also the degree of the integrated thermal storage. In addition, from the commercial experience to draw one, estimated land for solar thermal power plant is very hard to prepare. The

various existing land requirement for the solar thermal power plants are arrange in tabular form in table.

Table 2: Suggestive land area demand for solar thermal power plant [22]

Solar thermal power plant	**Land area (m^2)**	**Specific land area (m^2/kW)**	**Thermal storage (h)**	**Capacity (MW)**
Parabolic trough technology				
SEGS	6,400,000	18	-	354
Andasol	2,000,000	40	7.5	50
Nevada Solar One	1,600,000	25	-	64
Solnova	1,200,000	24	-	50
Solar tower technology				
Solar Tres	1,420,000	75	15	19
PS10	600,000	55	1	11
PS20	900,000	45	-	20

Chapter 3

MODELING THE PERFORMANCE OF PARABOLIC TROUGHS

3.1 Introduction

Parabolic trough collector is one of the most matured technologies for solar thermal power production. It takes the solar radiation and converts it heat transfer fluid which circulate through the thermal power cycle. In order to determine the useful energy obtained from a parabolic trough collector at a particular location, it is necessary to model the trough performance through a computer simulation on an hourly basis to understand what the annual performance will be.

3.2 Parabolic Trough Collector

The present study is concerned with the modeling of a cylindrical parabolic trough collector. The concentrating mirror has an aperture W, length L and rim angle ϕ_r as shown in Fig 3.1. The absorber tube consists of a steel pipe covered with a glass tube having inner diameter D_i and an outer diameter $D_o$respectively. The working fluid has a mass flow rate m, a specific heat C_p, inlet temperature T_i and outlet temperature $T_{o.}$

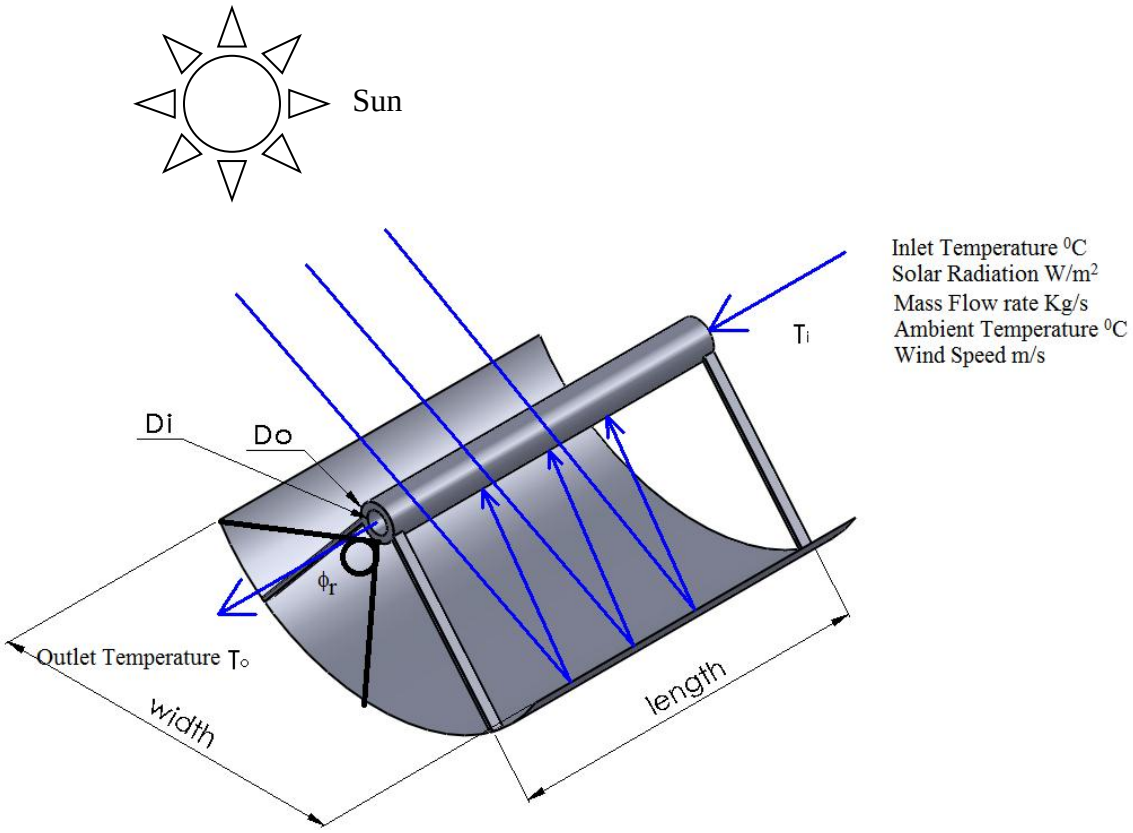

Fig 3.1: Information Flow Diagram for a Parabolic Trough Component

The collector operates in tracking mode with the beam radiation normally incident on its aperture. In some of the tracking modes, the sun's rays are incident at an angle and will therefore come to a focus little beyond the length of the concentrator. In this modeling, we assumed that the absorber tube is long enough to intercept this image.

This parabolic trough collector is modeled as a subsystem of a power plant. The required inputs for the trough model are the inlet fluid temperature (^{0}C), the solar radiation (W/m^2), the mass flow rate (Kg/s), the ambient air temperature (^{0}C), the wind velocity (m/s) and the trough size. The parabolic trough field model returns the outlet temperature, the absorbed radiation, energy loss and the efficiency of the collector field. The equations for the performance of a parabolic trough cannot be solved to find the

maximum parameters of a parabolic trough for the energy output; rather the equations describing a parabolic trough must be solved for each given set of parameter. The calculation for each parameter will be difficult to carryout manually. The use of simulation tool will be necessary to easily show the results for a given parameters.

3.2.1 Review of Simulation Models

Various numbers of simulations have been carried out on modeling the performance of parabolic trough with the aid of computer software. “Luz international limited developed an hourly simulation model that was used to help design the SEGS plants” [31] . Flabeg Solar international developed a performance simulation model to market parabolic trough plants and conduct design studies for clients” [32] . “KJC operating company (KJCOC), the operator of SEGS lll-lV, has developed an hourly simulation code for assessing the performance of its plants” [33] . “The German research laboratory Deutsches Zentrum Fur Luft-und Raumfarte.V (DLR) has also developed a performance model for parabolic trough plants” [34] . Most of these codes are owned by some organization and are not available to public. “DLR and Sandia National Laboratories (SNL) have developed a special library for use with the TRNSYS thermal simulation software, to model parabolic trough solar power plant” [35] . TRNSYS is commercial software and is appropriate for modeling complex software, like parabolic trough solar power plant. However, it is unfortunate that TRNSYS needs detailed input data to obtain results, which reflect on expected plant performance. “NREL developed a spreadsheet-based parabolic trough performance and economic model”[36].

3.2.2 Modeling with Visual Basic Excel

The simulation model used in the present work utilizes Viusual Basic built into Excel for programming the hourly performance. One of the main advantages of this approach

is that the user does not need special software to use the program. The key features of this simulation model are the solar radiation and the parameters of the parabolic tough added to the model, which optimized the parabolic trough design. This program runs through hourly values of different parameters contained in a Typical Meteorological Year (TMY) of North Cyprus. The Calculations to determine to end result of the solar field outlet temperature are described step by step in the following sections.

3.3 Optical Performance

3.3.1 Direction of Beam Radiation

The geometric relationship between the positions of the sun relative to the plane described in terms of several angles. The most important are:

Φ= latitude: Angular location between the north and south of the equator, north position $-90^0 \leq \varphi \leq 90^0$.

δ= Declination: The angle position of the sun at solar noon with respect to the plane of the equator is in Fig 3.2, north positive $-23.45^0 \leq \delta \leq 23.45$. In addition, it expressed in equation 3.3.

$$\delta = 23.45 \sin(360(284+n/365)) \qquad (3.1)$$

Where n=day of the year

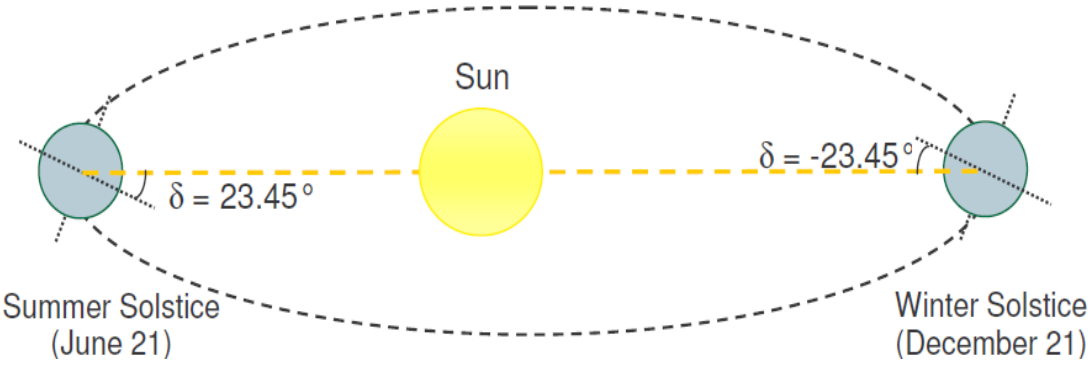

Fig 3.2: For a typical illustrated of the declination [49].

W= Hour angle: Angular displacement of the sum east to west of the local meridian due to rotation of the earth on its axis at 15^0 per hour, morning negative and afternoon positive. This described in equation 3.2.

$$(\text{Solar time} - 12) * 15^0/\text{hr} \qquad (3.2)$$

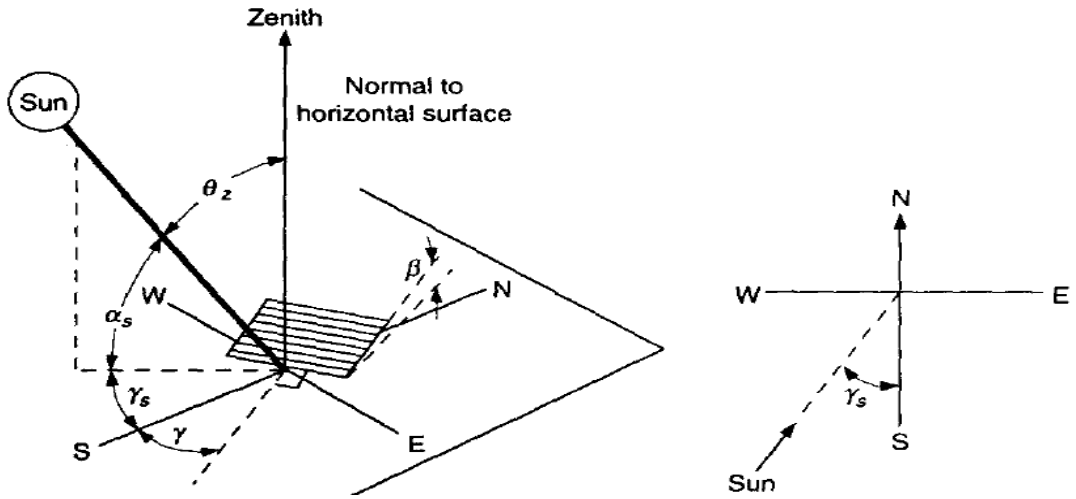

Fig 3.3: Zenith angle, slope, surface azimuth angle and solar azimuth angle for a tilted surface (b) plane view showing solar azimuth angle [9]

Θ_z= Zenith angle: The angle between the vertical and the line to the sun is described in Fig 3.3. given by equation 3.3

$$\theta_Z = \cos^{-1}(\cos(\phi) * \cos(\delta) * \cos(w) + \sin(\phi) * \sin(\delta)) \qquad (3.3)$$

Where

δ= declination angle

w= hour angle

Φ=latitude location of the plant

The slope of the parabolic trough at this given surface described in Fig 3.4 given by equation (3.4)

$$Tan\beta = \tan\theta_Z \left|\cos\gamma_S\right| \tag{3.4}$$

β= Slope: the angle between the plane of the surface in question and the horizontal, $0 \leq \beta \leq 180^0$ shown in Fig γ_s = solar azimuth angle

The solar azimuth angle for this mode of direction will change between 0 and 180^0 in Fig3.7. If the solar angle passes through $\pm 90^0$ for either hemisphere, then

$$\begin{cases} \left|\gamma_S\right| \leq 90, \gamma = 0^0 \\ \left|\gamma_S\right| \geq 90, \gamma = 180^0 \end{cases} \tag{3.5}$$

Thus, to calculate γ_s, we must know in which quadrant the sun will be. This determined by the relationship of the hour angle (w) to hour angle w_{ew}, when the sun is due west (or east). A general formulation for γ_s from [37], is conveniently written in terms of γ_s', a pseudo solar azimuth angle in the first or forth quadrant.

$$\gamma_S = C_1 C_2 \gamma_S' + C_3 \left(\frac{1 - C_1 C_2}{2} \right) 180 \tag{3.6}$$

Where γ_s'=pseudo solar azimuth angle.

$$\gamma_S' = \sin^{-1}\left(\frac{\sin w \cos\delta}{\sin\theta_Z} \right) \tag{3.7}$$

$$C_1 = \begin{cases} 1 if \left|w\right| \prec w_{ew} \\ -1, otherwise \end{cases} \tag{3.8}$$

$$C_2 = \begin{cases} 1 if\ \phi(\phi - \delta) \geq 0 \\ -1, otherwise \end{cases} \quad (3.9)$$

$$C_3 = \begin{cases} -1, if w \geq 0 \\ -1, otherwise \end{cases} \quad (3.10)$$

$$w_{ew} = \cos^{-1}\left(\frac{\tan\delta}{\tan\phi}\right) \quad (3.11)$$

Where w_{ew}=hour angle when sun is due east (or west)

If $\left|\frac{\tan\delta}{\tan\phi}\right|$ is greater than 1, the sun is never due east or west of the observer [9].

3.3.2 Angle for Tracking Surfaces

Parabolic trough directed with its focal axis pointed in the east - west or in the north-south direction. In the east-west orientation in Fig 3.4, the focal axis is horizontal, while in the north-south orientation, the focal axis may be horizontal or inclined. There are various tracking mode. But, for the case of simulation of parabolic trough in North Cyprus, a plane rotated about east-west with continuous adjustment to minimize the angle of incidence was selected because of the high concentration of beam radiation in the region [9].

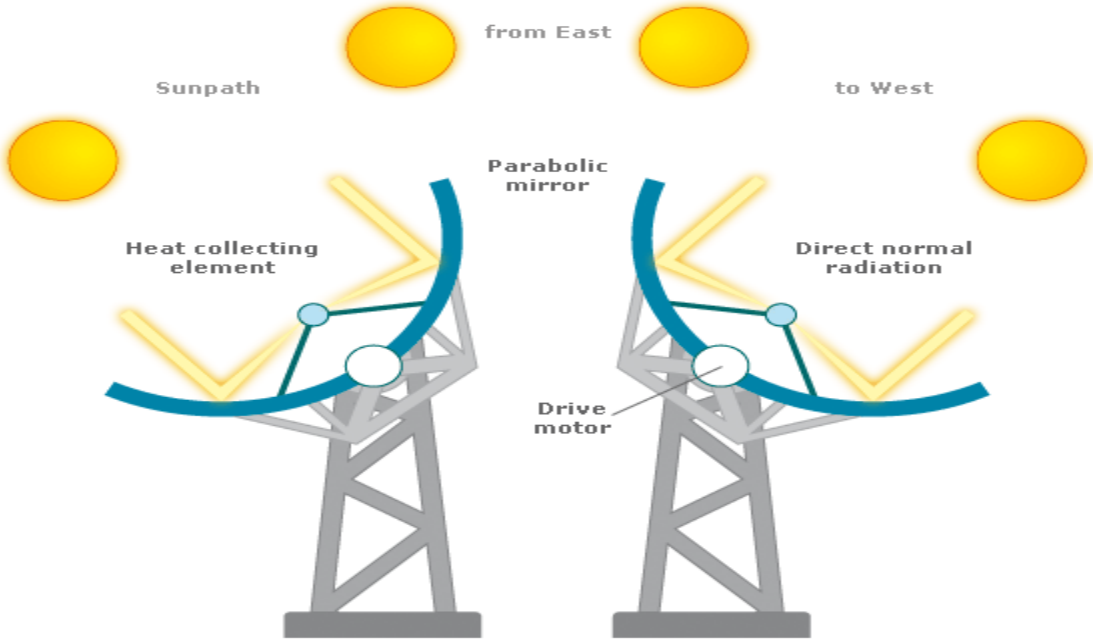

Fig 3.4: Schematic of Parabolic Trough Solar Tracking System [51]

3.3.2.1. Angle of Incidence (θ)

This angle of incidence of beam radiation on the aperture plane throughout the day is in equation (3.12). Fig 3.5 described the angle of incidence.

$$\theta = \cos^{-1}(1-\cos^2\delta * \sin^2 w)^{\frac{1}{2}} \qquad (3.12)$$

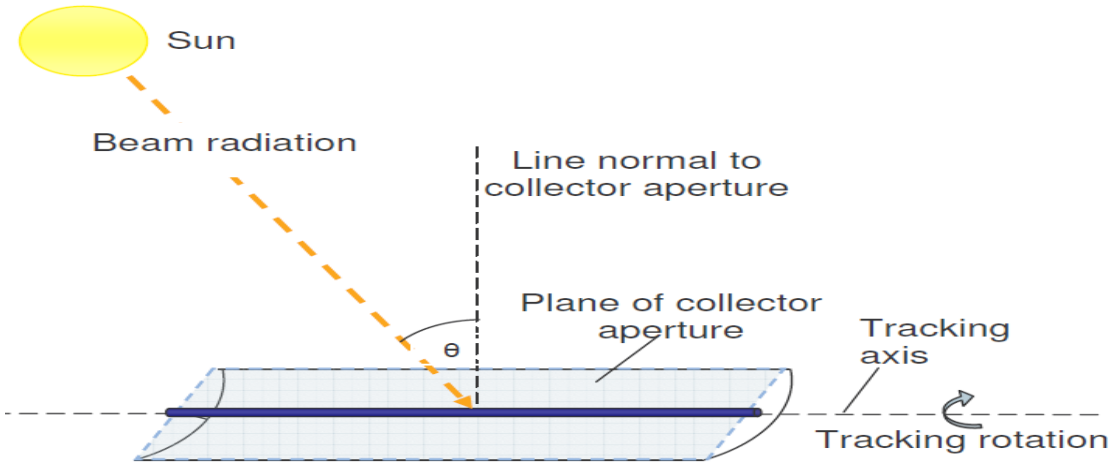

Fig 3.5: Pictorial of angle of incidence on the a parabolic trough [49]

3.3.2.2 Beam Radiation

The ratio of the beam radiation flux falling on a tilted surface to that falling on a horizontal surface in Fig 3.6. It denoted by R_b in equation 3.13.

$$R_b = \frac{\cos\theta}{\cos\theta_z} \tag{3.13}$$

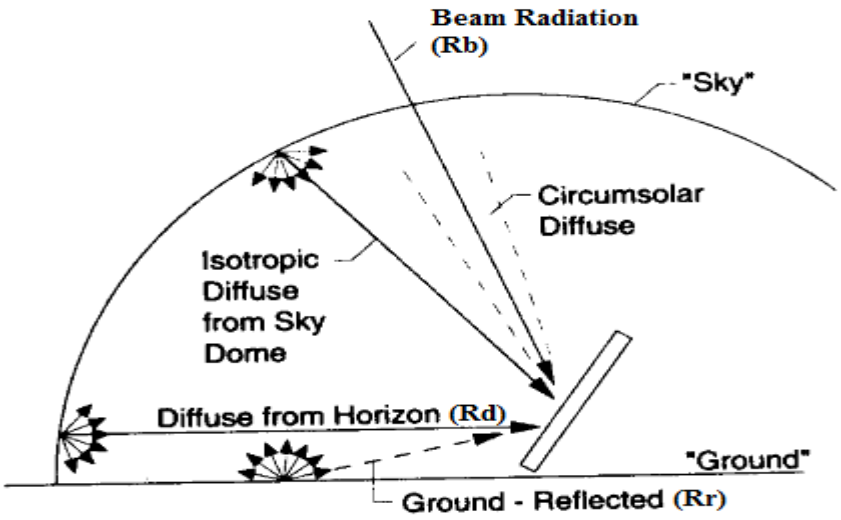

Fig 3.6: Beam, Diffuse and Ground-Reflected radiation on a tilted surface [9].

3.3.2.3 Diffuse Radiation

The tilt factor R_b for diffuse radiation is the ratio of the diffuse radiation flux falling on the tilted surface to that falling on a horizontal surface in Fig 3.10. The value of this tilt factor depends upon the distribution of diffuse radiation over the sky on the portion of the sky dome seen by the tilted surface. Assuming that the sky is an isotropic source of diffuse radiation, we have equation (3.14)

$$R_d = \frac{1+\cos\beta}{2} \tag{3.14}$$

β =slope

3.3.2.4 Reflected Radiation

Assuming that the reflection of the beam and diffuse radiation falling on the ground is diffuse and isotropic, and that the reflectivity is ρ, the tilt factor for reflected radiation is given by equation 3.15, described in Fig 3.10.

$$R_r = \rho\left(\frac{1-\cos\beta}{2}\right) \tag{3.15}$$

ρ=reflectivity

3.3.2.5 Flux on tilted surface

The flux l_T falling on a tilted surface at any instant thus given by equation 3.16

$$l_T = l_b R_b + l_d R_d + \left(l_b + l_d\right) Rr \tag{3.16}$$

Where the value of R_b, R_d and R_r are as given in equation 3.13, 3.14 and 3.15.

Equation 3.4 used in finding the slope of the aperture plane at any time it should be noted in this simulation; this is valid for south-facing surface.

3.3.3 Absorbance Collector Pipe

The absorbance surface of a collector is dependent on the incidence of the solar ray of the surface. The ratio of angular absorbance to normal absorbance is described in Eq. 3.17 for incidence angles betwixt 0 & 80^0.

$$\frac{\alpha}{\alpha_n} = 1 + 2.0345e^{-3}\theta - 1.990e^{-4}\theta^2 + 5.324e^{-6}\theta^3 4.799e^{-8}\theta^4 \tag{3.17}$$

θ =is in degree

For the final absorbance beam specular (α) of the pipe absorber is to multiply the ratio of Eq. (3.17) with the normal specular absorbance coefficient.

3.3.4 Transmission, Reflection and Absorptance of a Single Cover System

3.3.4.1 Transmissivity Based on Reflection – Radiation

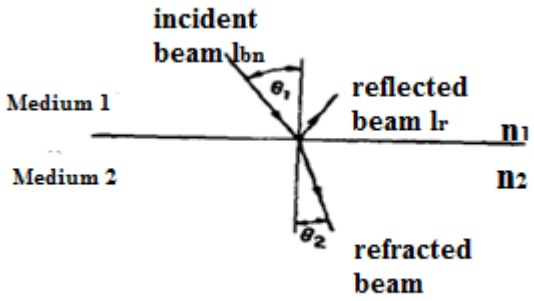

Fig 3.7 Angle of incidence and refraction at the interface of two media [9]

when a beam of light of intensity I_{bn} travelling through a transparent medium 1strikes the interface separating it from another transparent medium 2, it is reflected and refracted in Fig 3.7. The reflected beam has a reduced intensity I_r and has a direction such that the angle of reflection is equal to the angle of incidence. Therefore the refraction angle between the glass and the air interface can be calculated by equation (3.18).

$$\frac{n_1}{n_2} = \frac{\sin(\theta_2)}{\sin(\theta_1)} \qquad (3.18)$$

Where refractive index of air n_1 equals one assumed and n_2 is the refractive index for the glass, $\theta_1 = \theta$(Angle of incidence), θ_2 = angel of refractive.

For the special case of normal incidence ($\theta_1=0^0$), it can be shown that the reflectivity ρ can be described in equation (3.19) [12].

$$\rho = \left(\frac{n_1 - n_2}{n_1 + n_2}\right)^2 \qquad (3.19)$$

For a smooth glass, Fresnel has derived expression for the reflection of unpolarized radiation on passing from medium 1 with a refractive index n_1 to medium 2 with refractive index n_2 [9]

The perpendicular component of unpolarized radiation is described in equation (3.20)

$$r_{\perp} = \frac{\sin^2(\theta_2 - \theta_1)}{\sin^2(\theta_2 + \theta_1)} \tag{3.20}$$

Equation (3.21) described the parallel component of unpolarized radiation

$$r_{\Pi} = \frac{\tan^2(\theta_2 - \theta_1)}{\tan^2(\theta_2 + \theta_1)} \tag{3.21}$$

The parallel and perpendicular refer to the plane defined by the incident beam and the surface normal. A single glass cover system is adopted for trough simulation, equation (3.22) give the reflection of unpolarized radiation as the average of two components.

$$\tau_r = \frac{1}{2} * \left(\frac{(1 - r_{\Pi})}{(1 + r_{\Pi})} + \frac{(1 - r_{\perp})}{(1 + r_{\perp})} \right) \tag{3.22}$$

τ_r = Transmissivity obtain by considering only reflection and refraction

3.3.5 Absorption by Glazing

The absorption radiation in a partially transparent medium described by equation (3.23)

$$\tau_a = \frac{l_{transmitted}}{l_{incident}} = \exp\left(\frac{-K * L}{\cos\theta_2} \right) \tag{3.23}$$

K= coefficient extinction of glass

L = thickness of glass cover

τ_a = transmissivity obtained by considering only absorption.

3.3.6 Transmissivity of Cover System

According to Duffie [9], transmissivity of the cover system of a collector can be obtained with adequate accuracy by considering reflection-refraction and absorption separately, and is given by the product form in equation (3.24). It is also a satisfactory relationship for solar collector with cover materials and angles.

$$\tau = \tau_a * \tau_r \tag{3.24}$$

Out of the fraction τ transmitted through the cover system. A part is absorbed and a part reflected diffusely. Out of the reflected part, a portion is transmitted through the cover system and a portion reflected back to the absorber plate. The process of absorption and reflection at the absorber tube surface goes indefinitely, the quantities involved being successively smaller. Thus, the net fraction absorbed in shown in equation (3.25) [8]

$$(\tau\alpha)_b = \frac{\tau\alpha}{1-(1-\alpha)\rho_d} \tag{3.25}$$

The symbol ρ_d represents the diffuse reflectivity of the cover system. For a single cover system value for ρ_d can be shown to be 0.15.

3.3.7 Intercept Factor

The intercept factor for a linear imaging concentrator (as is the case for the parabolic trough) is the fraction of the reflected radiation that is incident on the absorbing surface of the receiver. For a receiver of large enough diameter, the fraction of the reflected radiation is 1.0. For a perfect linear imaging concentrator, the diameter ($D_{\Upsilon=1}$) of the cylindrical receiver for an intercept factor (Υ) equal to 1.0, which is described by equation (3.26). For a non-perfect imaging concentrator (defects in the surface of the reflector), the diameter ($D_{\Upsilon=1}$) is described by (3.26).

$$D_{\gamma=1} = w \times \frac{\sin(0.267)}{\sin(\phi_r)} \tag{3.26}$$

$$\phi_r = \tan^{-1}\left(\frac{8 \times \left(f/w\right)}{16 \times \left(f/w\right)^2 - 1}\right) \tag{3.26a}$$

$$D_{\gamma=1} = w \times \frac{\sin(0.267 + \delta_d/2)}{\sin(\phi_r)} \tag{3.27}$$

Where w is width of the aperture, f is the focal length of the aperture, and δ_d is the dispersion angle. For the simulation, the trough is assumed to be imperfect, meaning that the dispersion angle is greater than zero. The intercept factor was thus chosen for the simulation as described in equations (3.28)

$$\gamma = \begin{cases} 1 if D_0 \geq D_{\gamma=1} \\ D_0 / D_{\gamma=1} \; if D_0 \prec D_{\gamma=1} \end{cases} \tag{3.28}$$

Where $D_{\Upsilon=1}$ is given by equation (3.27)

It is worthwhile to note that using the proportion $D/D_{\Upsilon=1}$ for the intercept factor is very conservative for the second case of equation (3.26) since the distribution of radiation is theoretically a normal distribution.

3.3.8 Overall Optical Efficiency

The overall optical efficiency is the combination of the efficiencies from the cover transmission, collector absorptance, and the primary mirror reflectivity. This is shown in equation (3.29)

$$\eta_0(\theta) = \rho_e \times \alpha \times \tau \times \gamma \tag{3.29}$$

3.3.9 Absorbed Radiation

The prediction of collector performance requires information on the solar energy absorbed by the collector absorber plate. This is the actual quantity of radiation on the receiver and is calculated by equation (3.30)

$$S = I_b R_b [\rho\gamma\tau\alpha] + \frac{\tau\alpha D_o}{W - D_o} \tag{3.30}$$

Where, l_b =incident radiation, R_b =beam radiation, ρ =specular reflectance, γ =intercept factor, τ =transmittance, α =Absorptance, D_0=Outer diameter

3.3.10 Heat Loss by Radiation

In this section, there are two radiation coefficients calculated for a single system with a glass cover. The natural convection heat transfer coefficient $h_{r,r\text{-}c}$ for the enclosed annular space between a horizontal absorber tube (receiver) and a concentric cover is calculated by a given equation (3.31)

$$h_{r,r-c} = \sigma * \frac{(T^2{}_r + T^2{}_c) * (T_r + T_c)}{\frac{(1-\varepsilon_r)}{\varepsilon_r} + \frac{1}{F_{12}} + \frac{(1-\varepsilon_c) * D_o}{\varepsilon_c * D_c}} \tag{3.31}$$

Where T_r = Temperature of the receiver (absorber tube) (C)

T_c = Temperature of the cover (C), ε_r = = Emittance of the receiver (absorber tube),

ε_c = Emittance of the cover , D_0= Outer diameter of the receiver , D_c=cover diameter, F_{12}=view factor between the receiver and the cover (assumed to be 1), σ =Stefan Boltzmann constant (5.67E-8).

From equation (3.31), it was noted that the temperature of the receiver and cover temperature must be known to calculate the radiation coefficient. In the simulation, logical estimate was made at the average receiver temperature for the evaluation length by equation (3.31a) [9].

$$T_r = T_{in} + 0.25 * S * \left(\frac{(a - D_c) * l_{eval}}{m * C_p} \right) \qquad (3.31a)$$

Where l_{eval} = Evaluation length of the trough (m), m =mass flow rate (kg/s), C_p=specific capacity (KJ/Kg.k), D_c= Cover temperature, S= Absorber Radiation. (W/m), T_{in}= inlet temperature (K)

In the simulation, the cover temperature assumed 50% different between the receiver temperature and the ambient as illustrated in equation (3.31b). To determine the cover temperature second iteration of the thermal losses performed using the adjusted temperature cover.

$$T_c = 0.5 * (T_r - T_a) + T_a \qquad (3.31b)$$

For the second radiation coefficient between the cover and the ambient air is given by equation (3.32).

$$h_{r,c-a} = 4 * \sigma * \varepsilon_c * T_{loc}^{\ 3} \qquad (3.32)$$

Where T_{loc} =average (local) temperature between the cover and the ambient air=0.5*(T_c+T_a), and ε_c =is emittance of the cover.

3.3.11 Convection to Ambient

Determination of the convection to ambient is complex because the fluid dynamic will call for laminar or turbulent flow over the cover pipe depending on the Reynolds

number (Re). The equation for the convection coefficient is described in equation (3.33) [9].

$$h_w = \frac{Nu_a * K_a}{D_c} \tag{3.33}$$

K_a=thermal conductivity, Nu_a=Nusselt number of air, D_c= Cover diameter.

For flow of air across a single tube in an outdoor environment, the equations recommended by [38] modified to give.

$$Nu = 0.4 + 0.54 * \mathrm{Re}_a^{0.53} \; for 0.1 < \mathrm{Re}_a < 1000 \tag{3.33a}$$

And

$$Nu_a = 0.3 * \mathrm{Re}_a^{0.6} \; for 1000 < \mathrm{Re}_a < 50000 \tag{3.33b}$$

$$\mathrm{Re}_a = \frac{\rho_a * V_a * D_c}{\nu_a} \tag{3.33c}$$

Where K_a=thermal conductivity of air, V_a=velocity of air, D_C= Cover diameter. ν_a =Kinematic Viscosity of air

The air characteristic K_a, ρ_a and ν_a depends on the air temperature. Hence, the simulation incorporate these characteristics from [9] appendixes.

3.3.12 Overall Loss Coefficient and Cover Diameter

In this section, the procedure for calculating the overall loss coefficient U_L and the correlation required for calculating the individual heat transfer coefficients. The calculation of overall loss coefficient based on convection and re-radiation losses alone. For the top loss coefficient, we consider the absorber tube and the glass cover around it

to constitute a system of infinitely-long concentric tubes and is calculated by equation (3.34) [9].

$$U_L = \left(\frac{D_o}{(h_w + h_{r,c-a}) * D_c} + \frac{1}{h_{r,r-c}} \right)^{-1} \quad (3.34)$$

Where U_L=overall loss coefficient (W/m^{2}K), h_w=wind heat transfer coefficient (W/m^{2}K), D_c=cover diameter (m)

3.3.12.1 Cover Diameter

Evaluation of cover temperature performed in order to balance the energy on the cover by equation (3.35)

$$T_c = \frac{D_o * h_{r,r-c} * T_r + D_c * (h_{r,c-a} + h_w) * T_a}{D_o * h_{r,r-c} + D_c * (h_{r,c-a} + h_w)} \quad (3.35)$$

For the thermal losses and overall loss coefficient, a second iteration performed in the simulation with the adjusted cover temperature. Iteration results found satisfactory for the overall loss coefficient, extra iteration estimated unnecessary.

3.3.13 Convective Heat Transfer Coefficient

The heat transfer fluid in the receiver pipe (Water or HTF) described by turbulent or laminar flow conditions. Therefore, the Reynolds number of the fluid (Re_f) was evaluated in the simulation in equation (3.36a) and if then statement was used between equation (3.36b) for turbulent flow and (3.36c) for laminar flow to calculate the Nusselt number of the fluid (Nu_f) [9]. The coefficient of the heat transfer fluid (h_f) evaluated by equation (3.37)

$$Nu_f = \frac{(f/8)*\mathrm{Re}*\mathrm{Pr}}{1.07+12.7*\sqrt{(f/8)}*\left(\mathrm{Pr}^{2/3}-1\right)}*\left(\frac{\mu}{\mu_w}\right)^{n}1 \qquad (3.36)$$

For $\mathrm{Re}_f \succ 2200$

$$\mathrm{Re}_f = \frac{4*m}{\pi*D_i*\mu} \qquad (3.36a)$$

$$f = (0.79*\ln \mathrm{Re}-1.64)^{-2} \qquad (3.36b)$$

$$Nu = 3.7\ for\ \mathrm{Re} < 2200 \qquad (3.36c)$$

$$h_f = \frac{Nu_f * k_f}{D_i} \qquad (3.37)$$

Where Pr_f= Prandlt number of the fluid, μ_f = dynamic viscosity of the heat transfer fluid

μ_w = Dynamic viscosity of the wall temperature, m= Mass flow rate (Kg/s), D_i= Receiver inner diameter (m), h_f=Heat transfer coefficient of fluid, K_f=thermal conductivity of the fluid.

For laminar flow $\mathrm{Re}_f \prec 2200$, the hydrodynamic was fully developed and assumed the thermal profile. Since the $\mathrm{Re}_f \prec 2200$ the Nusselt number of the fluid was preferred to be 3.7 for the constant wall temperature rather than the 4.4 constant heat flux. The fluid water characteristic μ_w, μ_f, k_f and Pr_f are depended on the oil and water temperatures. Hence the simulation combined these featured from [9] and [39] appendix.

3.3.14 Overall Heat Transfer Coefficient and Factor

The overall heat transfer (U_o) is the coefficient of transfer of heat from surroundings to the fluid, station on the outer diameter of the receiver pipe. Duffie [9] gave the equation (3.38).

$$U_O = \left(\frac{1}{U_L} + \frac{D_O}{h_f * D_i} + \frac{D_O * \ln\left(\frac{D_O}{D_i}\right)}{2k} \right)^{-1} \tag{3.38}$$

Where K= thermal conductivity of receiver pipe.

3.3.14.1 Collector Efficiency factor

The collector efficient factor (F') can be defined by equation (3.39)

$$F' = \frac{U_0}{U_L} \tag{3.39}$$

3.3.14.2 Collector Heat Removal Factor

The term F_R is called the collector heat-removal factor described in equation 3.40. It is an important design parameter since it is a measure of the thermal resistance encountered by the absorbed solar radiation in reaching the collector fluid.

$$F_R = \frac{m * C_p}{A_r * U_L} * \left(1 - \exp\left(- \frac{A_r * U_L * F'}{m * C_p} \right) \right) \tag{3.40}$$

Where C_p=Specific heat of the fluid, A_r=Area of the receiver ($\pi D_0 LN$), L= length of receiver per module. N=number of modules.

The specific heat (C_p) depends on the HTF temperature. Equation (3.41) is a convenient expression for calculating the useful energy gain because the inlet fluid temperature is usually a known quality then, is calculated as described in [9] with equation (3.41)

$$Q = F_R * A_a * \left(S - \frac{A_r}{A_a} * U_L * (T_i - T_a) \right) \qquad (3.41)$$

Where A_a= Area of the aperture $((a - a_o)1N)$, a is the width of the aperture, a_0=is width of aperture shaded by the receiver, T=inlet fluid temperature (K).

3.3.15 Exit Temperature

Following the energy balance the exit temperature can be determine by equating the heat gained by the fluid to the useful heat gain rate, this can be described in equation (3.42) [8].

$$T_{fo} = T_f + \frac{Q_u}{mC_p} \qquad (3.42)$$

3.3.16 Efficiency of the Parabolic Trough

The parabolic trough efficiency is the amount of useful gain from the parabolic trough divided by the quantity of input energy to the parabolic trough. It was calculate in the simulation in equation (3.44)

$$\eta_{trough} = \frac{Q_u}{l_T A_a} \qquad (3.43)$$

Where A_a= Area of the aperture/reflector (m), Q_u=Useful gain for the trough for 1hour ($W/m^2.K$)

I_T=Flux incident on the top cover of the collector is given in equation (3.16) [8].

$$l_T = l_b R_b + l_d R_d + (l_b + l_d) R_r$$

l_b= Beam incidence (W/m^2), l_d=Diffuse incidence (W/m^2), R_b=Beam radiation, R_d=Direct beam radiation, R_r= Reflected radiation

Chapter 4

THERMAL PERFORMANCE OF A PARABOLIC TROUGH UNDER THE CLIMATIC CONDITIONS OF NORTH CYPRUS

4.1 Solar Radiation

The whole area of Cyprus has a mild climate with about 300days of sunshine with daily average solar radiation of about 5 kWh/m^2 on a horizontal surface. The solar energy input is particularly high at areas where the dry summer is well pronounced, lasting from April to October. In the lowlands the daily sunshine duration varies from 5.5 hours in winter to about 12.5 hours in summer. The mean daily global solar radiation varies from 2.3 kWh/m^2 in the cloudiest months of the year December and January, to about 7.2kWh/m^2 in July. The amount of global radiation falling on a horizontal surface with average weather condition is 1727 kWh/m^2 [40]. These values of solar radiation are quite high and consequently are very favorable for solar energy applications.

The solar radiation data used for the simulation model of a parabolic torugh collector were obtained by the meteorological Department (2004) of the North Cyprus. This data is fully presented at the appendix. The recording of the data were measured in 1hour intervals, at Ercan airport which have latitude of 35.09 degrees. The recording of the data were used by the pyranometer measured in cal/cm^2.

The direct solar radiation on horizontal surface is the only long term records measurement available in North Cyprus. However, in order to predict the energy delivery of any solar energy system, both the direct and diffuse component of solar radiation should be known. For this reason the diffuse component of solar radiation was estimated using the well know theories given in Duffie and Beckman [9]. The values of the daily hourly direct beam radiation in Ercan are listed in Table 4.1. The resulting hourly beam radiation data is the default input for the parabolic trough collector for a given day of the year.

Table 4.1: Shows the daily hourly analysis for average days for each months beam radiation l_b (W/m^2) for Ercan province for the year 2004

MONTH	DATE	8	9	10	11	12	1	2	3	4
January	27	112.81	169.8	406.1	315.	248.	225.6	315.8	315.	112.8
February	17	113.4	294.8	272.1	8	1	385.5	181.4	8	68.04
March	24	161.1	253.3	299.3	226.	136.	368.4	299.3	68.0	92.11
April	15	93.5	350.6	467.5	7	1	724.6	701.3	184.	537.6
May	15	187.9	352.3	446	333.	368.	728	728	2	610
June	14	407.2	527.0	674.0	7	4	790	767	631.	598.9
July	17	383.3	527.1	646.8	654.	710.	742.7	718.7	2	455.2
August	16	287.2	431.4	574.5	5	2	766.4	743.1	681	503.5
Septembe	28	215.6	359.3	479.1	610	681	622.9	574.9	718	335.4
r	29	117.4	258.4	399.3	724.	790.	93.97	187.9	598.	281.9
October	15	93.97	234.9	211.4	7	9	234.9	187.9	9	93.97
November	24	-	22.79	68.38	718.	766.	205.2	206.1	625.	91.2
December					7	6			3	
					671.	743.			479.	
					1	2			1	
					551.	622.			305.	
					0	9			4	
					305.	258.			140.	
					4	4			9	
					211.	375.			136.	
					4	8			7	
					136.	341.				
					7	9				

4.2 Performance Parameters

The simulation model parameters used in this study are shown in Table 4.2. Parts of these parameters were used in the calculation of the optical analysis. The rest were used as system parameters.

Table 4.2: The Simulation Input for the Parabolic Trough [48]

Solar Trough Concentrator	Values
Width (w)	5.77 (m)
Module Length (l)	6 (m)
Focal length (f)	1.71 (m)
Gap width (a_o)	0.1 (m)
Specific Reflectance (rs)	0.9
Number of modules (N)	1
Dispersion angle (D)	0.1degree
Solar Trough Receiver	
Cover diameter (D_c)	0.09 (m)
Receiver inner diameter (D_i)	0.05 (m)
Receiver outer diameter (D_o)	0.07 (m)
Absorber length (l)	12.5 (m)
Thermal conductivity of air (k_a)	0.026 (W/m.℃)
Thermal conductivity of steel	47.6 (W/m.℃)
Receiver emittance (ε_r)	0.91

Cover emittance (ε_C)	0.88
Cover thickness (L)	0.0025(m)
Cover extinction coefficient (K)	32(m^{-1})
Normal Specular absorbance α_n	0.93
Cover reflective index (n_2)	1.526
Heating Fluid (water =1,VP 1 Oil=2)	1
<u>Others</u>	
Latitude (Cyprus ,Ercan)	35^0, 09’
Day of the year (n)	Jan24,Feb17, March 26, April15,May15, Jun 11,Jul 17,Aug 16,Sept 28,Oct 29, Nov 14,Dec 24.
<u>Ambient conditions</u>	
Temperature (T_a)	298 (K)
Wind Velocity (V_a)	2.5(m/s)
<u>Fluid Conditions</u>	
Inlet temperature (T_i)	323 (K)
Mass flow rate (m)	0.07 (kg/s)

4.3 Simulation Results

The simulation model requires some input climatic weather data like the solar radiation, ambient temperature and wind speed. The Solar radiation is the most

influential of these data. Some selected days in each of the months of the year were used in the simulation. The performance of the system can be refereed by the variable inputed for the evaluation. The selected days chosen to determine the outlet temperature of the simulated parabolic trough reflected the sharp contrast in the weather condition from winter to summer seasons. The selected days for each month were the best pronounced weather condition for each month. The days are January 24, February 17, March 26, April 15, May 15, June 11, July 17, August 16, September 28, October 29, November 14 and December 24. The results of solar radition and resulted output temperature against time for each month are as shown in Figure 4.1 through 4.12.

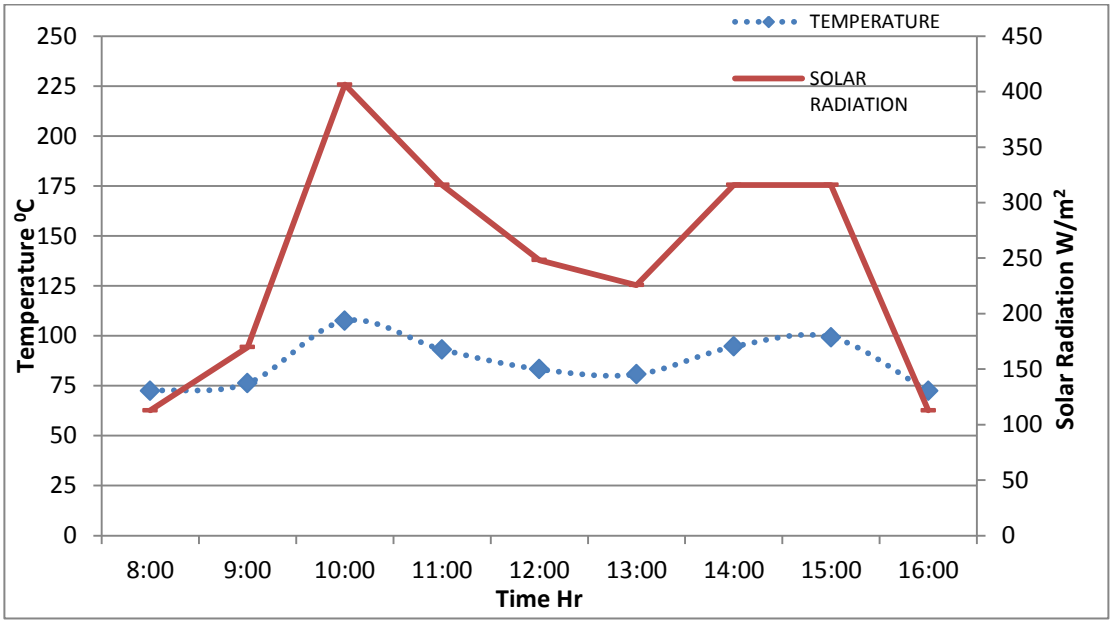

Fig 4.1: Solar Radiation and Heat Transfer Fluid Temperature for Cloudy period January 27, 2004

In Figure 4.1, the solar radiation shows mixed data of both clear and cloudy day. The expected maximum solar radition should occur around noon but in this Fig 4.1 it did occur around 10:00am. The day would have produced a better output temperature if the trend of the solar radiation was continued. The sharp decline from 10:00am could only

suggest a cloudy period of the day that was for about 4 hours. We can see that in the later hours of the day an increase in solar radition observed but the sun was ready to set.

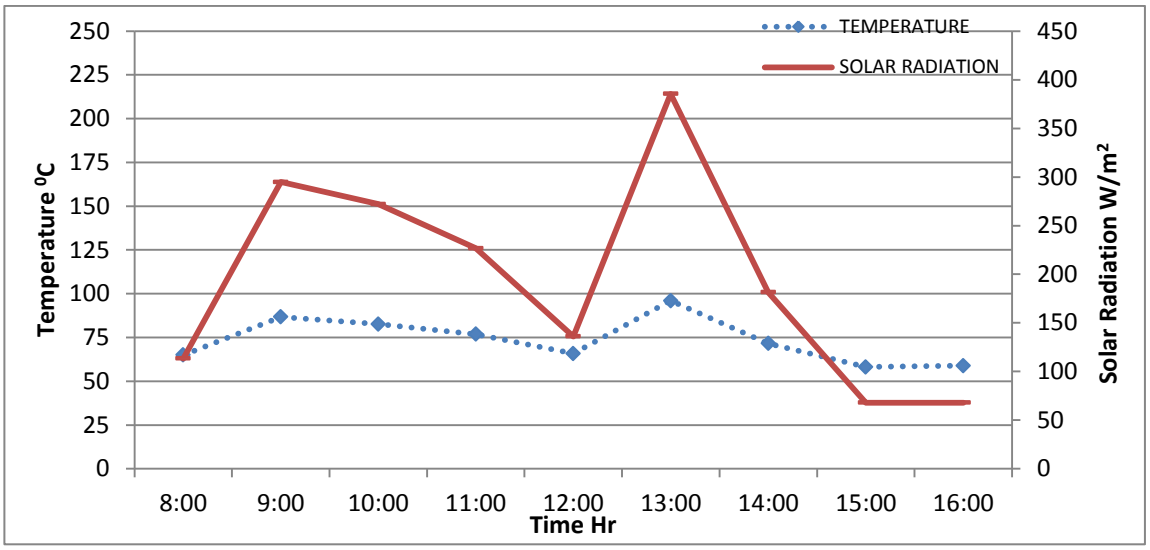

Fig 4.2: Solar Radiation and Heat Transfer Fluid Temperature for Cloudy period Febuary 17, 2004

In Fig 4.2, it was observed that the solar transient caused by the cloudy form explain the rise and fall of the temperature in the system. The maximum solar intensity obtained for this model occurs at 13.00 hours. The heat gain by the absorber tube follows the tread of the solar radiation at that particular hour. When the solar radiation begins to decline between the 9.00am to 12.00pm in Fig 4.2, the performace of the system reduces.

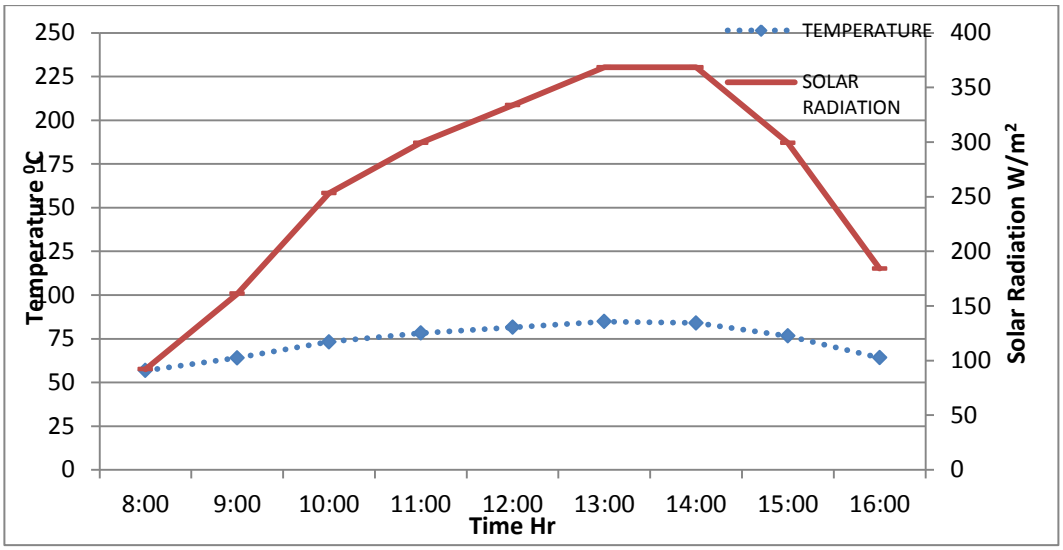

Fig 4.3: Solar Radiation and Heat Transfer Temperature for Rainy period March 26, 2004.

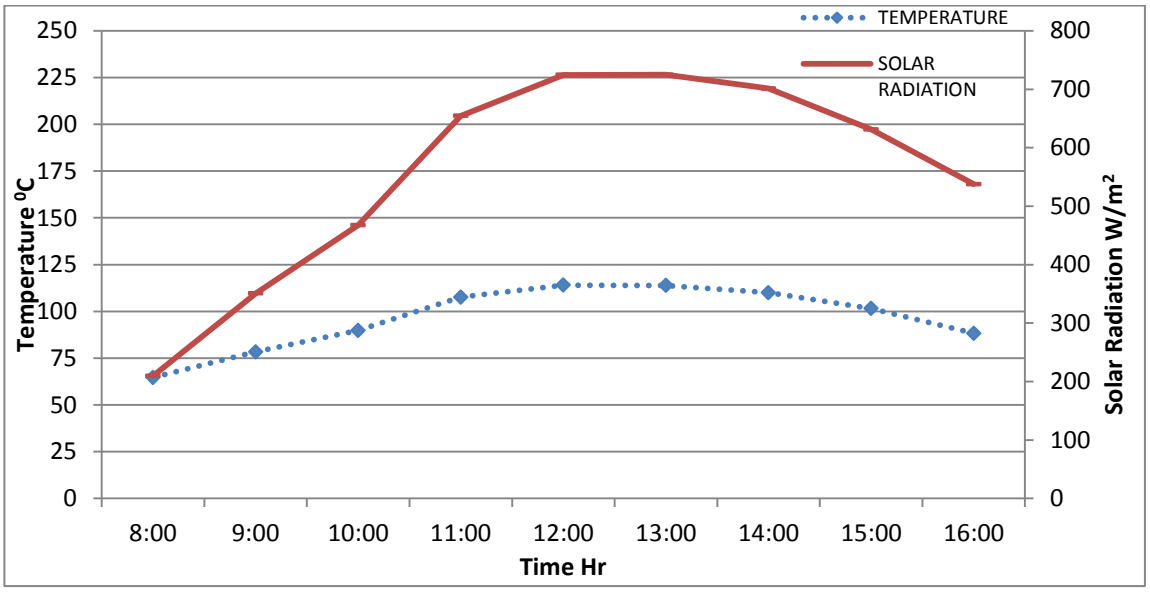

Fig 4.4: Solar Radiation and Heat Transfer Temperature for Sunny period April 15, 2004.

Fig 4.4 through 4.9 shows better solar radiation through the day. The days selected have clear weather and the solar radition figures are high. The high solar radition interpreted into high output of the system. It means that the system perfomed best with

this months with high solar radiation. The maximum solar radition for each month are there correspinding output temeperature.

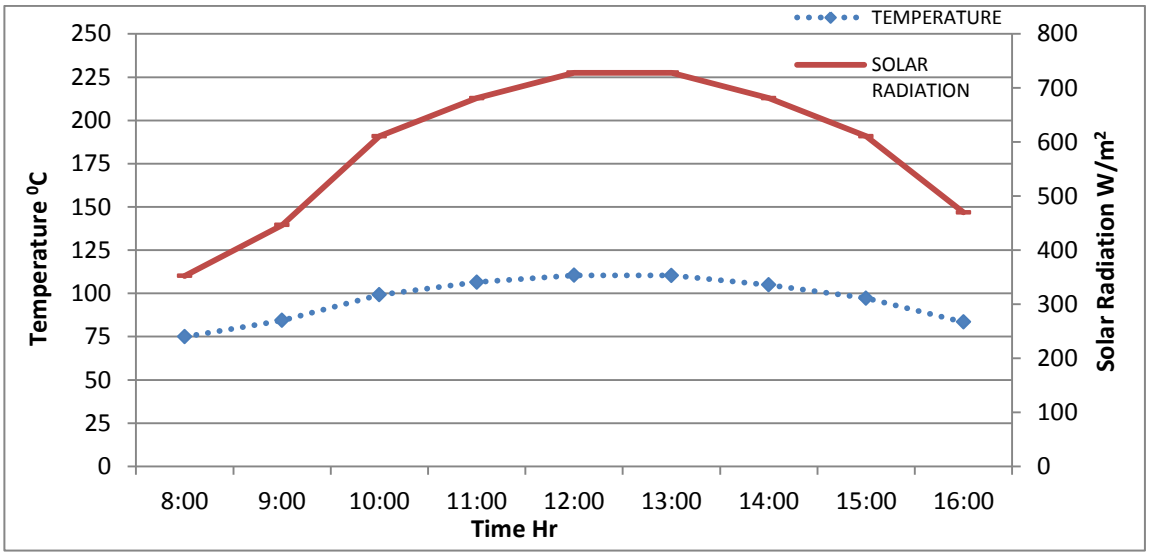

Fig 4.5: Solar Radiation and Heat Transfer Temperature for Sunny period May15, 2004.

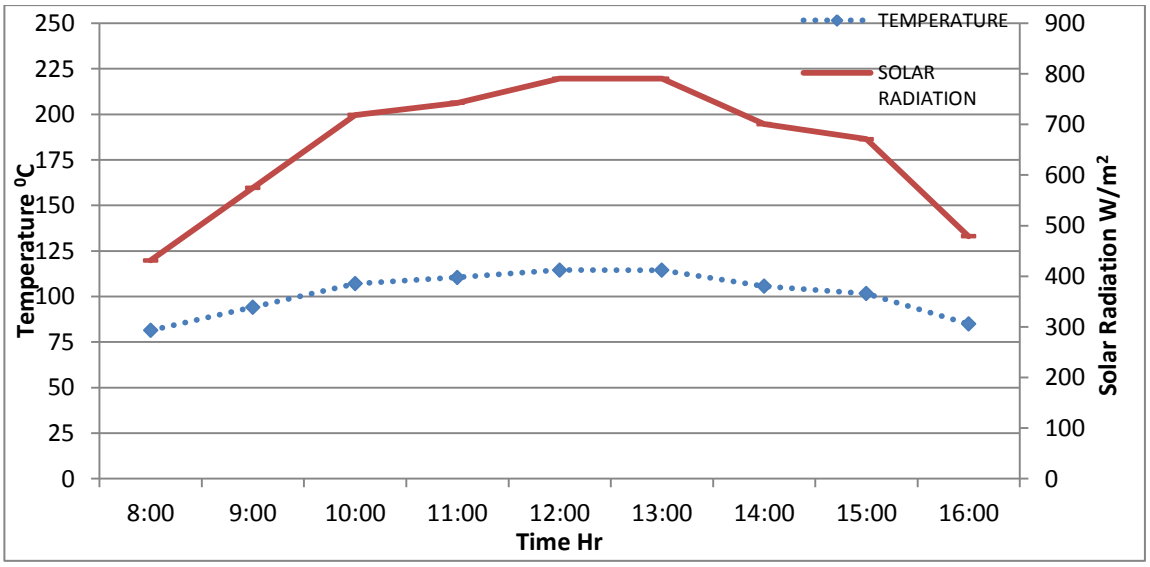

Fig 4.6: Solar Radiation and Heat Transfer Temperature for Sunny Period June 11, 2004.

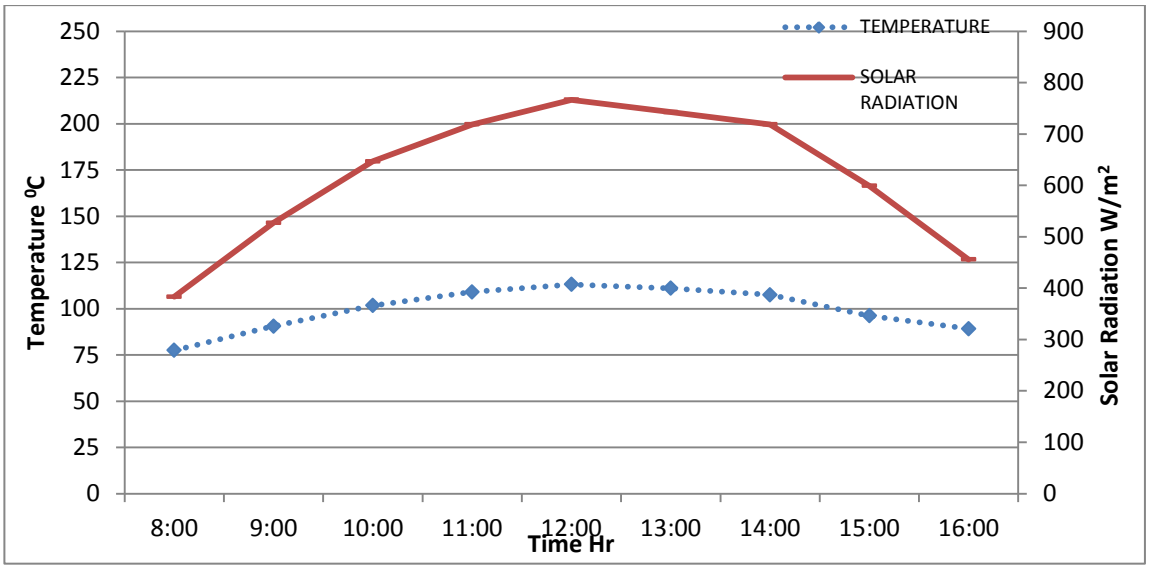

Fig 4.7: Solar Radiation and Heat Transfer Temperature for Sunny period July 17, 2004.

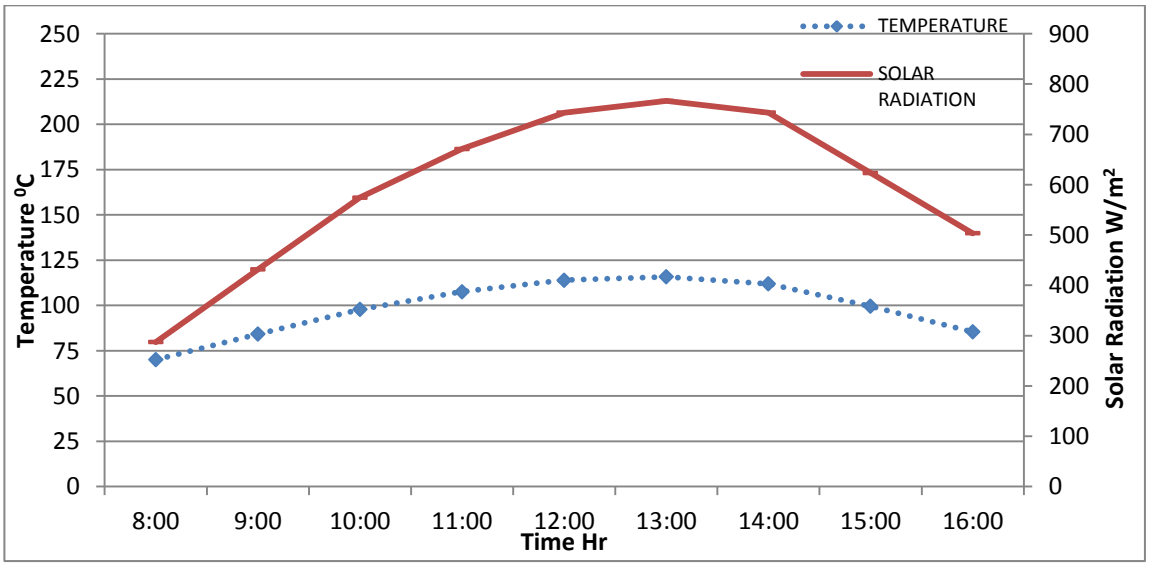

Fig 4.8: Solar Radiation and Heat Transfer Temperature for Sunny period August 16, 2004.

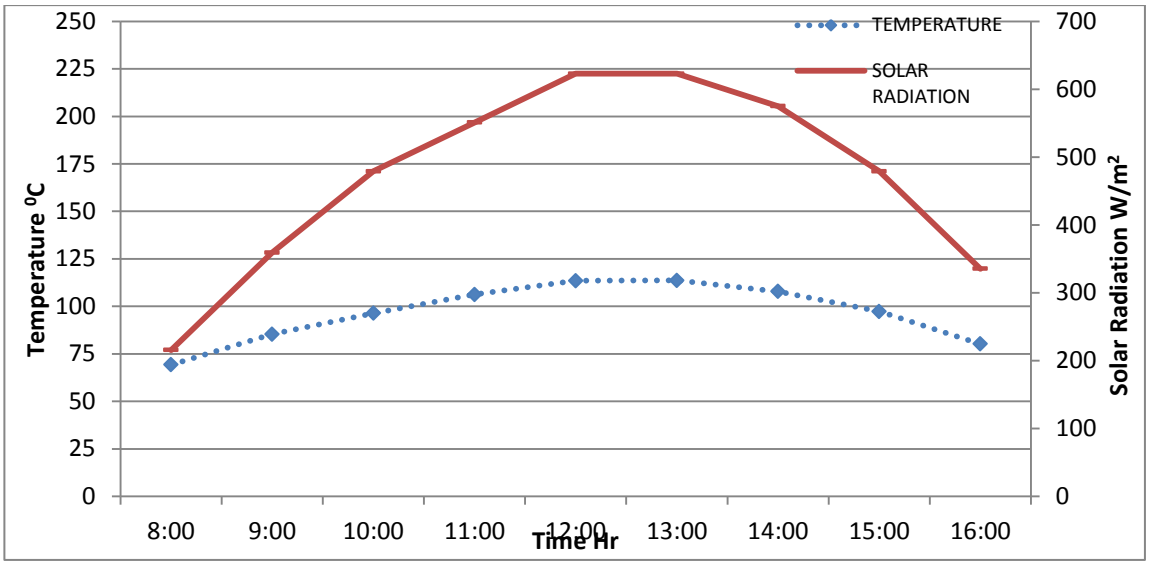

Fig 4.9: Solar Radiation and Heat Transfer Temperature for Sunny period September 28, 2004.

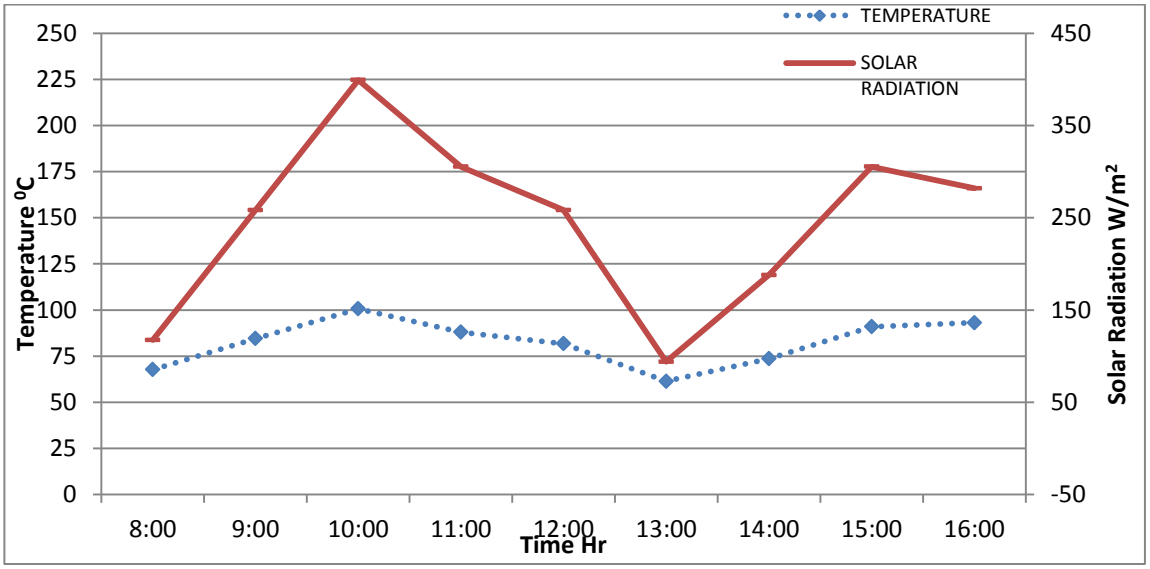

Fig 4.10: Solar Radiation and Heat Transfer Temperature for winter period October 29, 2004.

Fig 4.10 shows the solar intensity for all the day for the trough model. The solar intensity increased to the peak from the early hours of the days with 400W/m^2 at 10.00 am and decline at that same hour as a result of the solar transient.

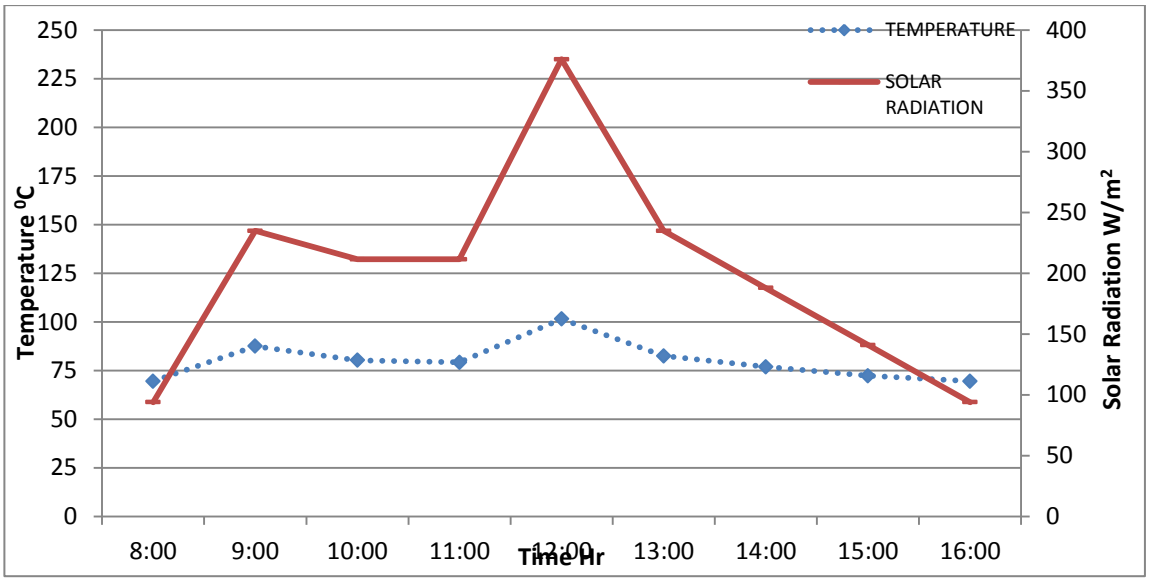

Fig 4.11: Solar Radiation and Heat Transfer Temperature for winter period November 15, 2004.

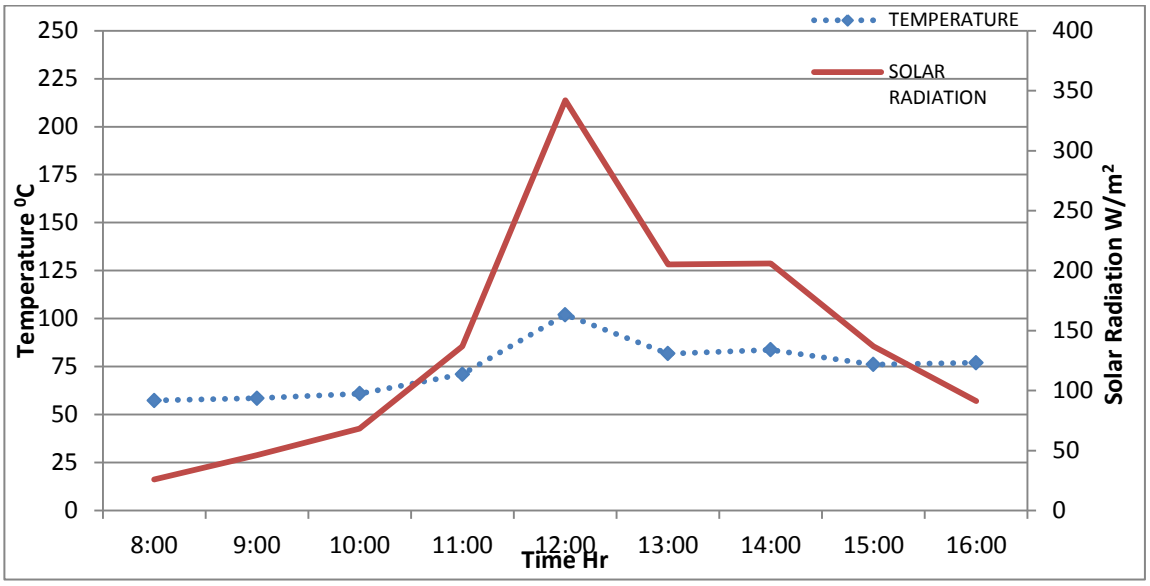

Fig 4.12: Solar Radiation and Heat Transfer Temperature for winter period December 24, 2004.

Fig 4.11 through Fig 4.12 demonstrated that the energy absorbed by the receiver tube is not retained by the heat transfer fluid due to losses in the radiation.

From the whole simulations analysis, it is shown that there are more solar radiation in the summer of year 2004 than the winter period.

Chapter 5

CONCLUSION AND RECOMMENDATIONS

5.1 Conclusion

The objectives of the present work are largely satisfied since a simulation of a parabolic trough is carried out under the climatic condions of North Cyprus. The simulation was able to estimate the temperature output for different months. Therefore it can be said that a useful tool was created for the purpose of studying or designing CSP plants using parabolic troughs.

5.2 Recommendations

Additional collection and process of solar data: the solar data that was used for the solar calculation has been gathered for the past 7 years. A credible solar radiation measuring system must be constructed in North Cyprus. There are various potential regions that seem to be appropriate examinee to conceal solar thermal power plants, yet they are not measured because there is no solar data valid for the regions.

- The use of solar data calculated in 5-10minute interval must be considered instead of the use of average monthly values for a particular hour. This will extremely increase the computed electrical power output and establish a favorably energetic variable into the analysis.
- The design study should evaluate the energy gain as a choice to increase output.

- During focusing on the parabolic trough technology, other technology should have a significant close watch on the development and their relative advantages. There would be leveraged in other technologies.
- Further investigation should include a vigorous simulation for the parabolic trough and a power plant model to be able to anticipate the system action under the climate of North Cyprus.

REFERENCES

1 Dr Henner Gladen. (2009). Solar Millennium A.G CUEN 3rd Annual Energy conference.

2 M. Petrakis, H.D. Kambezides, S. Lykoudis, A.D. Adamopoulos, P. Kassomenos, I.M. Michaelides, S.A. Kalogirou, G. Roditis, I. Chrysis and A. Hadjigianni. (2003). Data bank Generation of typical meteorological year (TMY-2) for Nicosia, Cyprus renewable energy. 28, 2317-2334

3 Greenpaces: solar thermal plant. (2008).

4 M. Ilkan, E. Erdil and F. Egelioglu. (2004). Renewable energy resources as an alternative to modify the load curve in Northern Cyprus. Energy. 30,333-372

5 S.Abbasoglu, U, Atikol, and N.Raheleh. (2010). Assessing the feasibility of a solar house in North Cyprus. 10th international conference on clean energy,

6 O.C Ozerdem, S .Biricik. (2011). Overview of energy system and major power quality problems in North Cyprus. Internal Journal on Technical and Physical Problems of Engineering (IJTPE). 3, 71-75

7 D.K.McDaniels, D.H. Lowndes, H.Mathew, J.Reynolds and R.Gray. (1975). "Enhanced solar Energy collection using reflector- solar thermal collector combinations" solar energy. 17, 277-285

8 S.P .Sukhatme. (1992). "Solar energy principle of thermal collection and storage" 6, 158.

9 John .A. Duffie, William .A. Beckman. (2006). "Solar Engineering of thermal processes".John Wiley and Son, 2006.

10 World Water & Solar Technologies Crop and Solargenix Energy, LLC sign strategic memorandum of understanding on sales and marketing efforts.

11 Philip Gleckman, Joseph O' Gallagher and Roland Winston. (1989) "Concentration of Sun Light to Solar Surface Levels Using Non- Imaging Optics". 31,198-200

12 R. Winston. (1970). "Light Collection within the frame work of Geometrical Optic. Working paper. 60,245-253.

13 J.F. Kreider, Charles .J.H. and Frank Kreith .Solar Design Components Systems Economics.McGraw-Hill.

14 Dr D.W Kearney. (2007), NREL, Parabolic trough workshop. Parabolic trough collector overview,

15 H. Price. (2003). NREL, International Solar Energy Conference. A parabolic trough solar power plant simulation model.

16 Black and Veatch. (February 9, 2005). New Mexico Concentrating Solar Plant Feasibility Study Draft Final Report. Prepared for New Mexico Energy, Minerals and Natural Resources Department.

17 C.Koroneos, P.Fokaidis, N.Moussiopoulos. (2003), Cyprus Energy System and the Use of Renewable Energy Sources. 40,1889-1901

18 J.M.Weungart. (1979). Global aspects of sunlight as a major energy source. Energy. 4,775-782.

19 Sergeant and Lundy LLC consulting group. (2003). Assessment of parabolic trough and power tower solar technology cost and performance forecast, Chicago, illinos, USA, NREL.

20 Concentrating Solar Power. (2007): Energy from mirrors. DOE/go-102001-1147FS128.

21 Shirish Garud Fellow and ishan Purohit, Research Associate. Making solar thermal power generation in India a reality- overview of technologies, opportunities and challenges. The energy and resources institute (TERI) India.

22 Andreas Poullikkas. (2009).Economic analysis of power generation from parabolic trough solar thermal plants for the Mediterranean region – A case study for the island of Cyprus. 13,2474-2484.

23 European Research on Concentrated Solar thermal energy European communities. (2004).

24 H.Muller- Steinhagen and F.Trieb. (2004). Concentrating solar power- A review of the technology ingenia, Royal Academy of Engineering, 18, 43-55

25 N. Bullard et al. (2008). Global Energy Supply Potential of Concentrating Solar Power, London.

26 S.Grama et al. (2008). Concentrating solar power- technology cost and markets. Prometheus institute for sustainable development, Chicago.

27 http://en.wikipedia.org/wiki/solar_energy_generating_systems

28 http:// www.flagsol.com/andasol_project_RD.htm

29 http://en.wikipedia.org/wiki/list_of_solar_thermal_power_stationsoperational .http://en.wikipedia.org/wiki/list_of_solar_thermal_power_stationsunderscon struction

30 Luz International Limited (LIL). (1990) “Solar Electric Generating System IX (SEGS IX) Project Description”. LIL Documentation, Los Angeles, CA.

31 Pilkington Solar International GmbH. (1996). “Status Report on Solar Thermal Power Plants”. Köln, Germany.

32 Nelson, R., and Cable, R. (1999). “The KJC Plant Performance Model – An Improved SEGS Plant Simulation”. Proceedings of the ASES 1999, Annual Conference.

33 Quaschning, V., Kistner, R., Ortmanns, W., Geyer, and M. (2001). “Greenius – A new Simulation Environment for Technical and Economical Analysis of Renewable Independent Power Projects,” Proceedings of ASME International Solar Energy Conference Solar Forum 2001. Washington DC, 34, 22-25

34 Jones, S., Pitz-Paal, R., Schwarzboezl, P., Blair, N., and Cable, R. 2001, “TRNSYS Modeling Of The SEGS VI Parabolic Trough Solar Electric Generating System,” Proceedings of ASME International Solar Energy Conference Solar Forum 2001. Washington DC. 5,22-25.

35 H.price. (March 16–18, 2003.). A Parabolic Trough Solar Power Plant Simulation Model. International Solar Energy Conference Hawaii Island, Hawaii

36 Broun, J.E and J.C Mitchell. (1983). Solar geometry for fixed and tracking surfaces. Solar energy. 31,439-449

37 Cengel Y.A and Turner RH. (2001): Fundamentals of thermal fluid scienes McGraw- Hill.

38 Metrological Service, Ministry of Agriculture and natural Resources of Cyprus: Solar Radiation and Sunshine duration in Cyprus. Cyprus, 1985.

39 Solar Radiation Map for European Countries: http://re.jrc.ec.europa.eu/pvgis/countries/Europe.htm#cy.

40 Frank van Mierlo, Breakdown of the incoming solar energy.jpg. http://en.wikipedia.org/wiki/file:breakdown_of_the_incomingsolar_energy.jpg

41 Wen Zhang. (2009) (Concentrating Solar power – state of the art, cost a study for the implementation China. Master Thesis.

42 H.J. Hou, Z.F Wang, R.Z. Wang, and P.M. Wang. (2005). A new method for the measurement of solar collector time constant. *Renewable Energy*, 30:855–865.

43 Y. Kim and T. Seo. (2007) Thermal performances comparisons of the glass evacuated tube solar collectors with shapes of absorber tube. *Renewable Energy*, 32:772–795.

44 P. Valera, A. Esteban, M. de los Reyes Carrillo, R Osuna, P. Menna, R. Gambi,P. Helm, M. Grottke, M. Geyer, F. Dobon, J. Monedero, A. Lugo, M. Romero, F. Chenlo, M. Alonso, M. Sanchez, J. Artigas, and A. Fresneda. Solar energy. (2003.) Comparative analysis of solar technologies for electricity production. *Proceedings of 3rd World Conference on Photovoltaic Energy Conversion*, 3,2482–2485,

45 Proceedings of Solar Forum (2001). Solar Energy: The Power to Choose. *TRNSYS Modeling of the SEGS VI Parabolic Trough Solar Electric Generating System*,

46 Conference Record of the IEEE 4thWorld Conference on Photovoltaic Energy Conversion. (2006). *Energy Performance Modeling of Stationary and Quasi-Stationary Solar Concentrators Based on Reverse Ray-Tracing Photovoltaic Energy Conversion*,

47 Eron Jacobson, Nipon ketjoy, Sukruedee Nathakaranakule and Wattanapon Rakwichian: Solar Parabolic Trough Simulation and Application for a hybrid power plant in Thailand.

48 A.M Pat node. (2006). Simulation and performance Evaluation of Parabolic Trough Solar Power Plants. Master's Thesis, University of Wisconsin-Madison.

49 Florides G, Kalogirou S.A. (2000). Modeling of the modern houses in Cyprus and Energy Consumption analysis. Energy, 25, 91-98

50 www.radiantandhydronics.com.

APPENDIX